Geological Quarterly, 2026, 70, 3
DOI: https://doi.org/10.7306/gq.1848

Palaeoenvironmental changes recorded in a fluviogenic peatland, inferred from subfossil Scots pine (*Pinus sylvestris*) dendrochronology and peat analysis: the Mosty site (Biała Nida River floodplain, southern Poland)

Włodzimierz MARGIELEWSKI[1, *], Marek KRĄPIEC[2], Krzysztof BUCZEK[1], Katarzyna KORZEŃ[3], Andrzej OBIDOWICZ[4], Artur GÓRECKI[5], Elżbieta SZYCHOWSKA-KRĄPIEC[2], Dariusz SALA[6], Jan URBAN[1] and Jolanta PILCH[1]

[1] Institute of Nature Conservation, Polish Academy of Sciences, al. A. Mickiewicza 33, 31-120 Kraków, Poland; ORCID: 0000-0002-6327-1217 [W.M.], 0000-0001-9501-0567 [K.B.], 0000-0002-6102-1599 [J.U.], 0000-0003-4033-1122 [J.P.]

[2] AGH University of Krakow, al. A. Mickiewicza 30, 30-059 Kraków, Poland; 0000-0003-4270-1668 [M.K.], 0000-0003-0809-8084 [E.S-K.]

[3] Kazimierza Wielkiego 110/2-3, 30-074 Kraków, Poland

[4] W. Szafer Institute of Botany, Polish Academy of Sciences, Lubicz 46, 31-512 Kraków, Poland; ORCID: 0009-0002-4242-4816

[5] Faculty of Biology, Jagiellonian University, Gronostajowa 3, 30-387 Kraków, Poland; ORCID: 0000-0002-0632-6074

[6] Institute of Nuclear Physics, Polish Academy of Sciences, Radzikowskiego 152, 31-342 Kraków, Poland; ORCID: 0000-0003-1723-0008

Margielewski, W., Krąpiec, M., Buczek, K., Korzeń, K., Obidowicz, A., Górecki, A., Szychowska-Krąpiec, E., Sala, D., Urban J., Pilch, J., 2026. Palaeoenvironmental changes recorded in a fluviogenic peatland, inferred from subfossil Scots pine (*Pinus sylvestris*) dendrochronology and peat analysis: the Mosty site (Biała Nida River floodplain, southern Poland). Geological Quarterly, **70**, 3; https://doi.org/10.7306/gq.1848

Associate Editor: Wojciech Granoszewski

The Mosty site, located in an abandoned meander of the Biała Nida River (southern Poland) includes fluviogenic peat 1.54 m thick, with a record of palaeoclimatic changes since the Boreal phase (9258 cal BP). During exploitation of peat and sand, numerous subfossil tree trunks, mainly Scots pine (*Pinus sylvestris* L.), were extracted from the deposits. Reconstruction of palaeoenvironmental changes on the basis of peat multiproxy analysis of lithology, plant tissues, pollen and non-pollen palynomorphs and geochemistry, together numerous radiocarbon dates and dendrochronological analysis of subfossil wood, indicates flood-derived clastic sediment input to the peatland at ~8.2 ka BP, at 6.8–5.3 ka BP, to lesser extent after 4.2 ka and ~2.8 ka BP, and since 1.522 ka BP. A sedimentary hiatus was probably related to the strong cooling and drying of the climate at ~4.2 ka, which caused a break in peat sedimentation. The oldest single pine tree trunks dated by ^{14}C at 10,198–9757 and 9426–9128 cal yrs BP grew as pine forest on the Biała Nida floodplain before the beginning of accumulation of the Mosty peatland deposits. A younger, single subfossil tree trunk (2964–2632 cal BP) grew in bog pine woodland on the peatland (above the hiatus) and fell during climate deterioration at ~2.8 ka. On the basis of the wiggle matching method, two bog pine floating chronologies were developed for the periods 1360–1187 (modelled age cal BP) and 1158–976 (mod. cal BP). The pine dying-off phase coincided with a significant increase in climate humidity in the 5th and 6th centuries AD, which included several fluctuations. The pine floating chronologies indicate the occurrence of alternating germination and dying-off tree phases. The beginning of colonization of the peatland by bog pines occurred during climatic drying, whereas the tree dying-off phases (deforestation) in peatlands took place during the climate humidity growth.

Key words: fluviogenic peatland, Holocene palaeohydrology, pine dendrochronology, peat multiproxy analysis, southern Poland

INTRODUCTION

Within the European peatlands, numerous subfossil trunks, extracted during peat exploitation, have been used both to develop chronologies (floating or absolute) and to help reconstruct

* Corresponding author, e-mail: margielewski@iop.krakow.pl
Received: November 18, 2025; accepted: February 3, 2026; first published online: April 7, 2026

palaeoclimatic (particularly palaeohydrological) changes during the Holocene based on peat multiproxy analysis. Usually, the tree species studied are Scots pine (*Pinus sylvestris* L.), and English oak (*Quercus robur*), other species being less commonly used (i.e. Gunnarson et al., 2003; Leuschner et al., 2007; Eckstein et al., 2008; Nicolussi et al., 2009; Edvardsson et al., 2016b, 2022; Árvai et al., 2016; Achterberg et al., 2017, 2018). To date, research on subfossil tree trunks has been conducted on peatland deposits in England, Scotland, Ireland, the Netherlands, Germany, Denmark, Sweden, Finland, Lithuania, regions of the Swiss and Austrian Alps, and the Romanian Carpathians (see also Edvardsson et al., 2016b). In Poland, such studies have covered 10 peatlands based on subfossil pine (*Pinus sylvestris*) and oak (*Quercus* sp.) trunks extracted during industrial peat exploitation or during fieldwork (Margielewski et al., 2022a, b, 2024).

Subfossil tree trunks are also frequent in alluvial deposits (Becker and Shirmer, 1977; Kalicki and Krąpiec, 1995; Kolář and Rybniček, 2011; Carozza et al., 2014). Dendrochronological analysis and dating of subfossil trunks of these trees has made it possible to document the formation, evolution and destruction of riparian forest vegetation (Finishinger et al., 2013; Lézine et al., 2013; Carozza et al., 2014). In Poland, one such locality with numerous subfossil tree trunks is the Mosty site, located in southern Poland at the southern margin of the Holy Cross Mts. (Fig. 1A, B). This is a fluviogenic peatland formed by paludification of an abandoned meander of the Biała Nida River. The periodic fluvial activity of the Biała Nida River strongly influenced the sedimentary record of this peatland. Peat deposits (minerogenic sedge peat) constitute the overburden of alluvial sands excavated commercially (Figs. 1E: 2 and 2A, B). Peat is also extracted during this exploitation and used for horticultural purposes. Numerous subfossil pine stumps extracted from the deposits during their exploitation have been subjected to dendrochronological analysis (Figs. 2A, B and 3A, B), while the peat deposits have been subjected to multiproxy analyses: lithological, telmatological (plant tissue analysis), palynological, and Non Pollen Palynomorphs (NPPs) (Figs. 4 and 5), as well as geochemical (Fig. 6). Radiocarbon dating of subfossil wood and peatland deposits was also performed (Figs. 2–4). This paper contributes to the reconstruction of Holocene climate changes based on the analysis of deposits from a fluviogenic peatland affected by periodic river activity and therefore prone to palaeohydrological fluctuations (Margielewski, 2022a). The main research question was therefore to determine the impact of fluvial activity on the record of palaeoenvironmental changes within this peatland. Our study utilized dendrochronological analyses of subfossil tree trunks buried in sediments, key issues being determination of the origin of the wood (riparian forest, driftwood, or bog pines) and reconstruction of the Holocene palaeohydrological (palaeoenvironmental) variability record inferred from the peat stratigraphy and subfossil tree trunk dendrochronology.

STUDY AREA

The Mosty peatland (GPS: N50°46,516'; E20°24,490'; 200 m a.s.l.) is located in southern Poland, at the southern margin of the Holy Cross Mts. (Fig. 1A). It was formed within the Biała Nida River valley (Nida Basin), on the Jędrzejów Plateau: the western, Cenozoic margin of the Kielce Upland (the SW margin of the Holy Cross Mts., Przedborsko-Małogoskie Range), and the western part of the Niecka Nidziańska Depression (according to Kondracki, 2000; see Kalicki and Biesaga, 2024; Fig. 1B, C).

The Nida River valley lies south of the Paleozoic core of the Holy Cross Mts. (Kowalski, 2002). From Chojna and Żerniki (Biała Nida River: see Fig. 1B and C) to Brzeźno (Nida River, after the confluence of the Biała and Czarna Nida), the Nida Valley was formed within the Mesozoic margin of the Holy Cross Mts., composed here of Upper Jurassic rocks, mainly limestones, some with flints (Hakenberg, 1974; Kowalski, 2002). Below the confluence of the Biała and the Czarna Nida rivers (outside the study area – see Fig. 1B), the Nida River valley traverses Cretaceous rocks of the Nida Basin (marls and limestones). In the study area, the bedrock of the Nida Basin is composed of Jurassic rocks forming a syncline, overlain by the Cretaceous strata noted above (Hakenberg, 1978), and in the lower course of the river (outside the study area) by Miocene deposits (limestones, sands, clays and gypsum). Quaternary deposits dominate the study area, their thickness ranging from a few to a ten or so metres (Hakenberg and Lindner, 1971). During the Pleistocene glaciations, the Nida Basin area was covered by ice sheets on several occasions (Lindner, 1978, 1982). As a result of their activity, fluvioglacial sediments (sands and gravels) and moraine clays were deposited, which today form a discontinuous sedimentary cover (Hakenberg, 1974; Rutkowski, 1986). The contemporary river valley floor forms a multi-stage floodplain with relative heights of up to 3 m (Fig. 1C, D). Numerous oxbow lakes of the Biała and Czarna Nida rivers, related to fluvial activity with varying degrees of channel development, are preserved on its surface (Fig. 1C, E; Krupa, 2013). In the interfluve of the Biała and Czarna Nida rivers, fluvial sands were reworked into aeolian dunes in the Younger Dryas Stadial (Krupa, 2013; Kalicki and Biesaga, 2024).

The study area generally comprises upland relief, while the Biała Nida valley separates two areas of different morphology. The area to the north of the river valley is characterized by small height differences and monotonous topography, while the southern part has diverse topography (uplands, hummocks, mesas, sills, plains and denudation basins, river terraces), reflecting greater lithological variability and rock weathering resistance (see Fig. 1C, D; Gilewska, 1972).

The average annual rainfall in the area between the Biała and Czarna Nida rivers is 650 mm, with the heaviest rainfall occurring in summer (Suligowski et al., 2009).

Forest cover in the Biała and Czarna Nida river basins does not exceed 25% (Krupa, 2013). The dominant vegetation types are subcontinental oak-hornbeam forests and continental mixed pine-oak forests. In the interfluve section of the Czarna and Biała Nida, riparian ash-elm forest occurs. Small areas are also occupied by sparse oak forest and fir forest (Matuszkiewicz et al., 1995). In the estuarine section of the Biała and Czarna Nida, aquatic, reed, and peatland vegetation communities occur, associated with peatlands (of minerogenic type) developed within the river valleys (Matuszkiewicz et al., 1995). Meadow communities occupy significant areas on the floodplain and low terraces (Krupa, 2013).

The Mosty peatland was formed on the outwash sand plains of the Odranian (Saalian) glaciation, within which the Nida River valley was formed. Later, the sands were reworked by the river in the Vistulian (Hakenberg, 1974; Kalicki and Biesaga, 2024). As already noted, the peatland is fluviogenic, formed by paludification of one of the abandoned meanders of the Biała Nida River, at its confluence with the Czarna Nida River (Fig. 1C, E). The peat deposits, recorded as ~1.54 m thick, constitute the overburden of the sandy fluvial deposits of the Biała Nida River, which are exploited commercially by the Organic Fertilizer Pro-

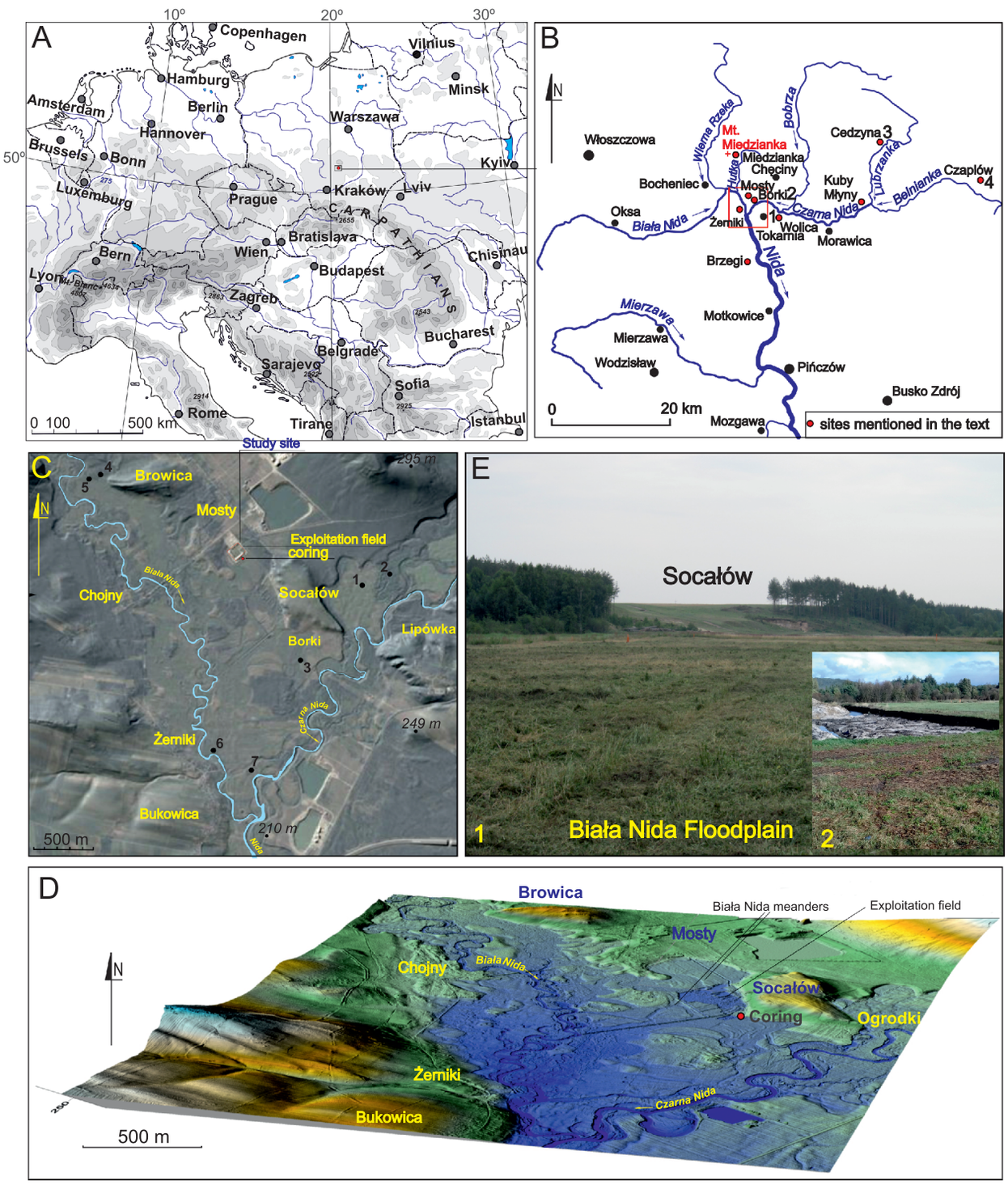

Fig. 1. Location of the Mosty site

A – in Europe and Poland; **B** – position in the Nida River catchment (red circles indicate sites mentioned in the text: site numbers: sites with subfossil trees shown in Fig. 7A); **C** – Shuttle Radar Topography Mission (SRTM) image of the interfluve region between the Biała Nida and Czarna Nida rivers, with location of exploitated areas and core site, sites 1–7 are mentioned in the text; **D** – LiDAR DTM of the interfluve area of the Biała and Czarna Nida rivers, with location of exploited areas and core site; **E** – Biała Nida floodplain (1), and exploitation scarp (2). Photos by W. Margielewski

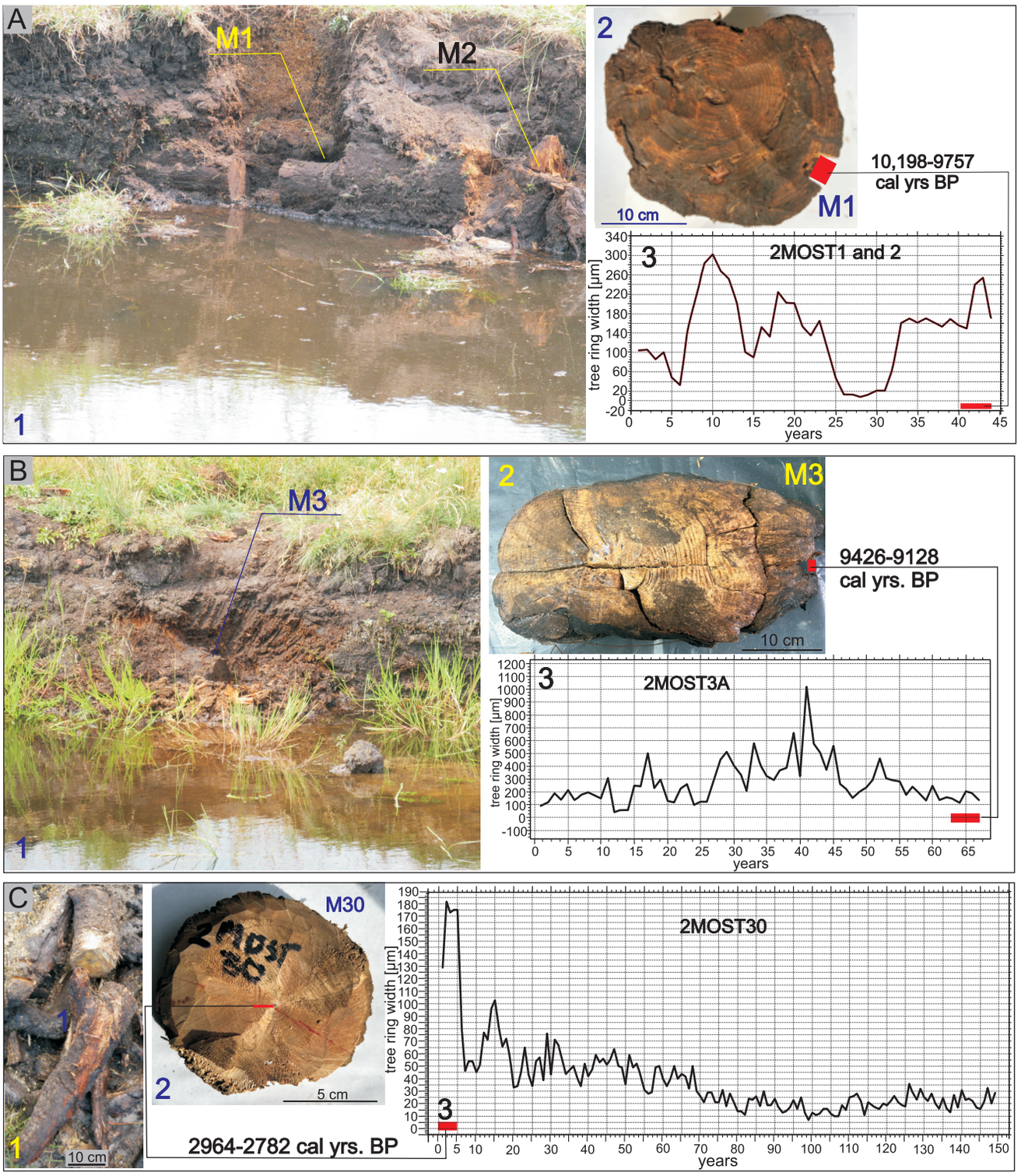

Fig. 2A, B – single subfossil pine tree trunks (*in situ* position), exposed and sampled directly in an exploitation scarp. 1 – fallen subfossil tree trunk (M1) and its butt end (M2) still rooted in bedrock; 2 – cross-section of the stem, 3 – averaged dendrochronological curve of a fallen tree trunk and its butt part (red colour – sample used for ^{14}C dating); B – fallen subfossil pine tree trunk (1 – M3), with cross-section (2) and its dendrochronological curve (3); C – subfossil pine tree trunk, excavated during exploitation (1), and its cross-section (2), its dendrochronologcal curve showing extremely thin tree rings. In this case, wood from the 5 first tree rings was dated (marked in red). Dendrochronological analysis by M. Krąpiec and E. Szychowska-Krąpiec. Photos by W. Margielewski

duction and Sand Mining Plant (Z.W.P. Mosty) in Chęciny (Figs. 1E: 2 and 3C). Within the peat, numerous subfossil tree trunks (including Scots pines *Pinus sylvestris* L.) are present (Fig. 2A, B), some having been excavated during mining (Figs. 2C and 3C–E).

MATERIALS AND METHODS

FIELDWORK AND SAMPLING: TREE TRUNKS AND DEPOSITS

Wood samples for dendrochronological analysis (trunk slices ~5 cm thick) were taken from the subfossil trunks using a gas-engine chainsaw Stihl (Figs. 2 and 3E). In total, 29 samples of wood of various species, including Scots pine (*Pinus sylvestris* L.) were collected. Wood samples were collected directly from exploitation scarps (Figs. 1E: 2, and 2A, B), as well as from stems occurring (*ex situ*) on a heap of excavated material located near the "ZWP Mosty" exploitation factory (Figs. 2C and 3C–E). The subfossil pine trees showed various trunk diameters, from 10 cm up to a maximum of 30 cm (Figs. 2 and 3E). Due to the state of preservation of the wood and its species diversity (including the genera *Salix*, *Betula* and *Pinus*), only well-preserved pine wood could be used for dendrochronological analysis: in total, 11 tree trunks were used to develop the floating chronology, all taken from the excavated heap (Fig. 3D–E). Individual tree trunks were also dated during this study (Fig. 2). Among the pine trunks occurring *in situ*, directly within the exploitation scarps (see e.g., Fig. 2A, B), some rested directly on the sand underlying the peat (Figs. 2A: 2 and 3B: 1). One of the trees was still rooted in the sandy substrate: its butt end (Fig. 2A: M2) and fallen trunk (Fig. 2A: M1, 3) were preserved. Numerous deciduous tree taxa (mainly *Salix*, less frequently *Alnus*) also occurred here, these being unsuitable for chronology. Furthermore, the poor state of preservation of the wood from some of the trunks prevented dendrochronological analysis. Although the age of three pine trunks was radiocarbon dated and subjected to dendrochronological analysis, this did not provide a basis for compiling another chronology (Fig. 2).

Drilling and core collection from the peatland deposits was carried out using a Russian sampler (INSTORF bit with diameters of 7 and 10 cm), directly in the area marked for exploitation, though in an area not yet disturbed (Figs. 1C, E and 3A). Samples of organic deposits were taken from the core at intervals of 2.5 and 5 cm and prepared for the following analyses: lithological (with loss on ignition), telmatological (plant tissue analysis), pollen and non-pollen palynomorphs (NPPs), and geochemical analysis. Many radiocarbon (^{14}C) dates: LSC (Liquid Scintillation Counting), as well as AMS (Accelerator Mass Spectrometry) were obtained from the peatland deposit sequence (Table 1). The sands underlying the peats were dated using the OSL method (Fig. 4A). Dates of subfossil wood (tree ring wood) were used for construction of floating chronologies (Fig. 3A, B and Table 1).

DENDROCHRONOLOGY (FLOATING CHRONOLOGIES)

Tree ring widths were measured (to an accuracy of 0.01 mm) in the Laboratory of Dendrochronology of AGH University of Krakow using *Dendrolab 1.0* equipment (Zielski and Krąpiec, 2004). The dendrochronological sequences were analysed using *TREE-RINGS* and *TSAP* software (Krawczyk and Krąpiec, 1995; Rinn, 2005).

The crossdates of wood samples were statistically validated, using the 'Gl coefficient' (Gleichläufigkeit; Eckstein and Bauch, 1969), and t-coefficient (Baillie and Pilcher, 1973). The accuracy of the measurements and the quality of the cross-dating were verified by *COFECHA* software (Holmes, 1999). The bog pine floating chronologies were constructed on the basis of relative age of wood, and by the wiggle-matching method using the *OxCal* (*v. 4.4.3*) computer program (Bronk Ramsey, 2009; Fig. 3A, B and Table 1).

DATES

Radiocarbon (^{14}C) conventional dates of organic material (peat, wood detritus) were prepared in the Laboratory of Absolute Dating in Krakow, Poland, using the LSC (liquid scintillation counting) method, according to the Krąpiec and Walanus (2011) procedure. Samples were chemically prepared using the acid-alkali-acid method (AAA), and the standard procedure of synthesis of benzene from carbonized samples (Skripkin and Kovalyukh, 1998).

A total of 7 ^{14}C dates of organic deposits (peat, wood detritus) and 7 dates of subfossil wood (selected tree ring sequences) were obtained (Figs. 2A, B, 3A, B, 4A and Table 1). They were used to date the floating chronologies of pines based on dendrochronological analysis and wiggle matching (Table 1). Radiocarbon dates were calibrated using the *OxCal* computer program *v. 4.4.3* (Bronk Ramsey, 2009, 2017) on the basis of the *IntCal20* radiocarbon calibration dataset (Reimer et al., 2020). After calibration, the dates were given as cal yrs. BP ages (with 95.4% probability; Table 1).

An absolute chronology for the sedimentary sequence was determined based on 7 LSC radiocarbon dates (Table 1). The age-depth model was calculated using the P_sequence function of *OxCal 4.4.3* software with the following parameters: k0= 0.95, log10(k/k0) = U(-1,1) and interpolation = 0.5 cm (Fig. 4B; Bronk Ramsey, 2009). The IntCal 20 atmospheric curve was used for calibration of dates (Reimer et al., 2020). A major lithological change, reflecting the transition between sedge peat and organic silt (recorded at 60 cm) was introduced to the age-depth model using Boundary command (Bronk Ramsey, 2009). The age for the sedimentary sequence is reported as the mean (μ) value derived from the age-depth model, with associated uncertainty expressed as ±1σ, in modelled calibrated years before present (mod. cal BP). The sedimentary accumulation rate (AR) was calculated based on the age-depth model (mm yr^{-1}) (Fig. 4B).

Dating of the sands beneath the peat was carried out using the OSL method in the laboratory of the Jan Kochanowski University in Kielce.

LITHOLOGICAL AND PLANT TISSUE ANALYSES

Loss on ignition (LOI) analyses were prepared for each 2.5 cm interval of the lithological sequence (Fig. 4A, C). Each sample was dried and subjected to ignition in a muffle furnace at 550°C for 4 hours (Heiri et al., 2001). On the basis of LOI analysis of 56 samples, a loss on ignition curve was produced in depth interval (Fig. 4A) as well as in time interval (Fig. 4C) context: the second using *Tilia Graph* software (Grimm, 1987, 1991).

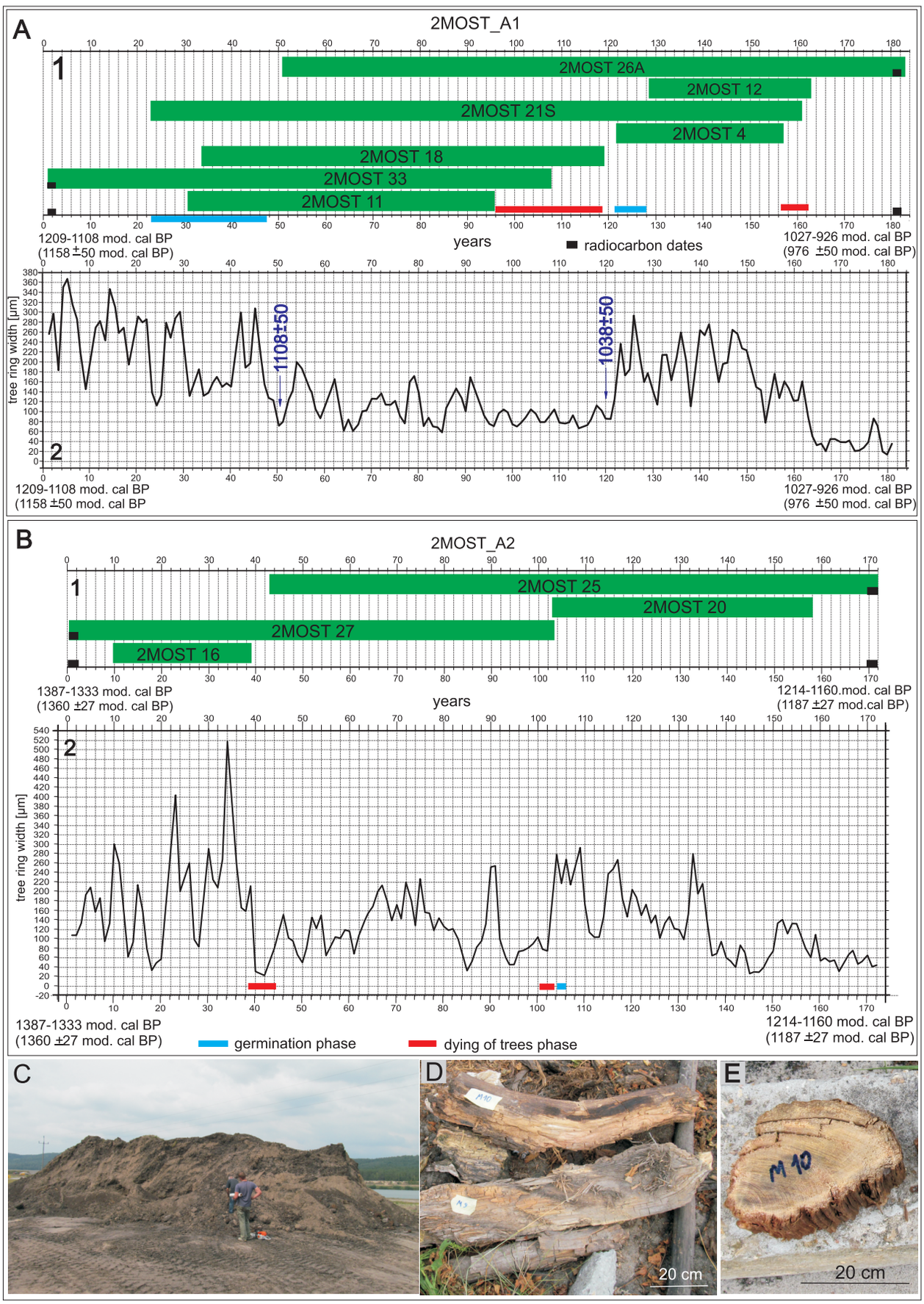

Fig. 3A, B – pine (*Pinus sylvestris*) floating chronologies of subfossil trees excavated in the Mosty peatland (A1 and B1) on the basis of dendrochronological analysis and wiggle matching, with averaged dendrochronological curves for each chronology (A2 and B2) (analysis by M. Krąpiec and E. Szychowska-Krąpiec); C – post-exploitation heap of excavated sand, with subfossil tree trunks (D and E). Photos by W. Margielewski

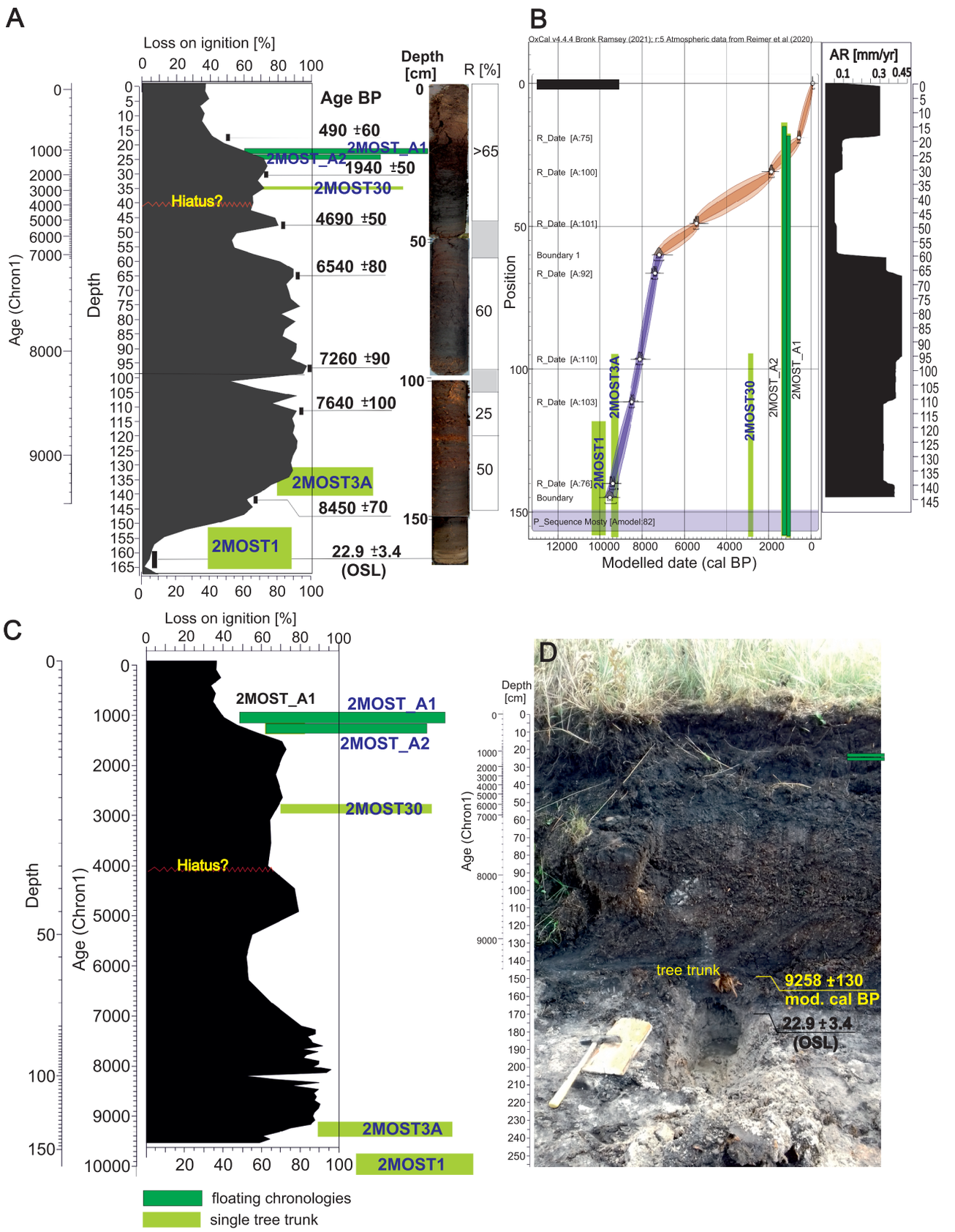

Fig. 4. Sedimentary sequence of the Mosty peatland

A – loss on ignition curve of the deposits (shown on a depth scale), with radiocarbon dates and the modelled age scale (on the left); photo of log made using the Instorf drill-bit (on the right), and factor (indicator, degree) of peat decomposition (R – constructed by A, Obidowicz); **B** – age-depth model (constructed by K. Buczek), with accumulation rate of deposits [in mm yr^{-1}]; **C** – loss on ignition of deposits shown on an age scale; **D** – photo of sedimentary sequence of the Mosty peatland. Time-range of floating chronologies and position of dated tree trunks are shown in green. Photos by W. Margielewski

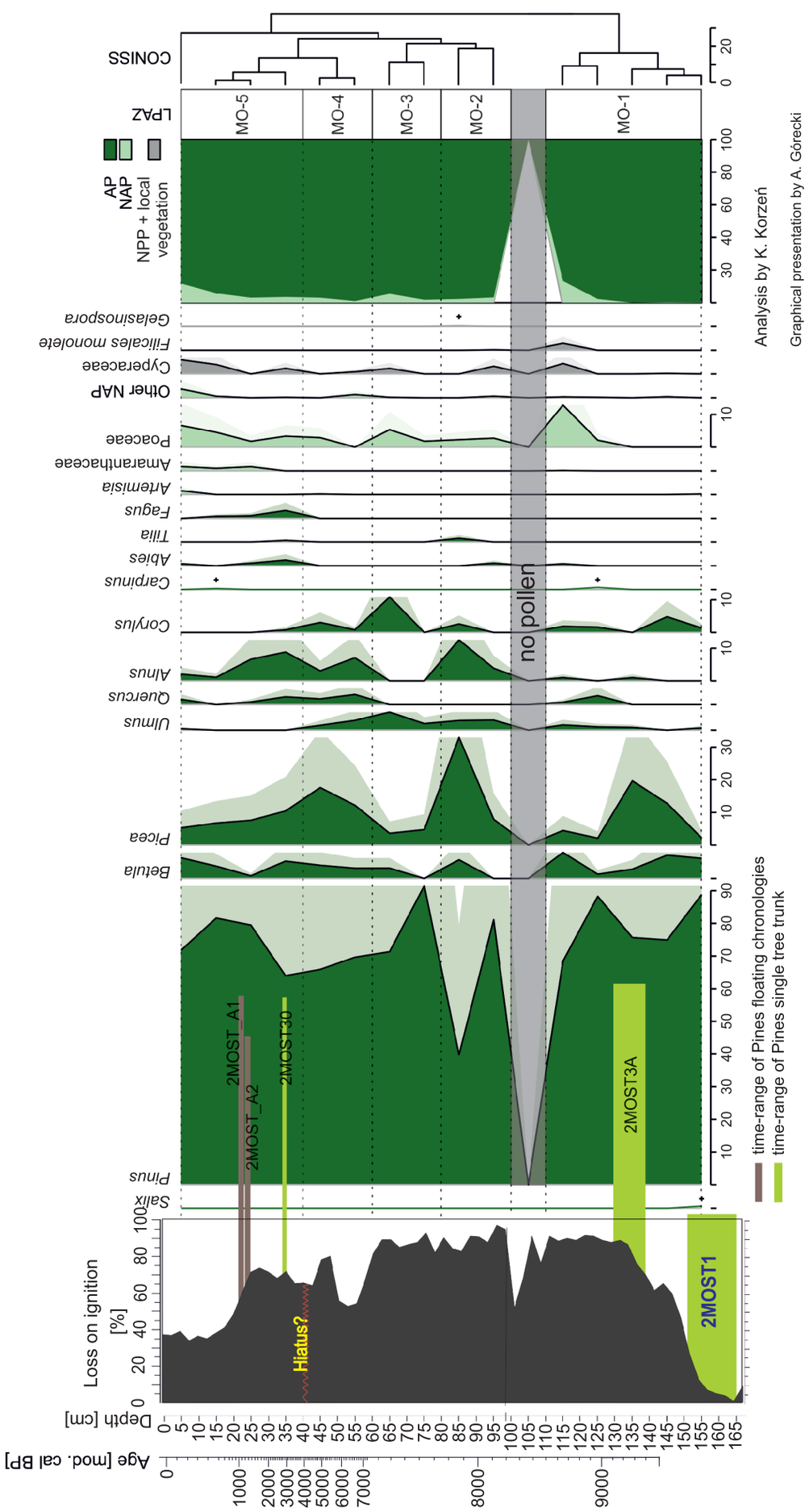

Fig. 5. Percentage pollen diagram of the Mosty peatland deposits

Analysis by K. Korzeń, statistical analysis and graphic presentation by A. Górecki

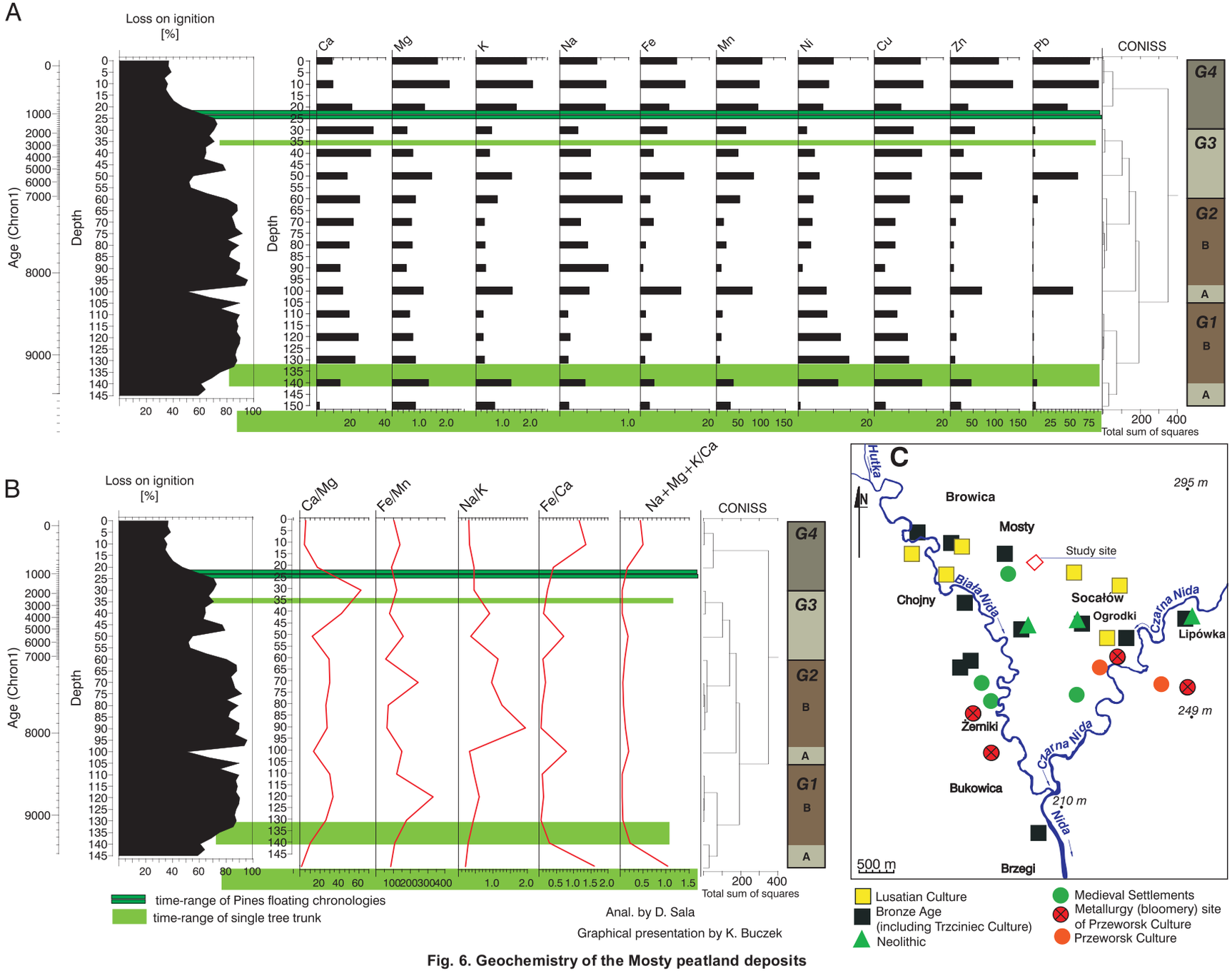

Fig. 6. Geochemistry of the Mosty peatland deposits

A – content of the major elements; **B** – geochemical indicators (analysis by D. Sala; statistical analysis by K. Buczek), with position of subfossil trees; **C** – archaeological sites in the interfluve area of the Biała Nida and Czarna Nida rivers, with sites with metallurgy activity (bloomers) [according to the Archaeological Picture of Poland (AZP): after Krupa, 2013; Kalicki and Biesaga, 2024]

Table 1

Radiocarbon dates of peat and tree trunk wood (the last one for wiggle matching), as well as an OSL date of sand in the Mosty peatland

Depth [cm]	Material	Lab. code	Age ^{14}C [yrs BP]	Calendar age 2σ [cal. yrs BP]
17.5–20.0	peat	MKL-6997	490 ±50	634–590 (10.3%) 563–456 (84.6%) 348–341 (0.6%)
30.0–32.5	peat	MKL-4738	1940 ±50	1990–1958 (6.9%) 1950–1736 (88.5%)
47.5–50.0	peat	MKL-6998	4690 ±60	5894–5806 (16.7%) 5792–5787 (0.4%) 5767–5588 (78.4)
65.0–67.5	peat	MKL-4737	6540 ±80	7575–7307 (94.3%); 7295–7282 (1.2%)
95.0–97.5	peat	MKL-4736	7260 ±90	8319–8245 (5.9%) 8218–7931 (88.7%) 7891–7875 (1%)
110.0–112.5	peat	MKL-4735	7640 ±100	8635–8616 (1%) 8605–8280 (88.9%) 8269–8195 (5.7%)
140.0–145	peat	MKL-4044	8450 ±70	9543–9395 (78.7%) 9387–9296 (16.7%)
110	quartz grains OSL Date	UJK-OSL-101	22.9 ±3.4 ka	–
Wood dated for wiggle matching				
2MOST21AW	pine wood	MKL-4195	1200 ±30	1244–1214 (5%) 1179–1057 (88.3) 1022–1006 (2.1%)
2MOST25B z30	pine wood	MKL-5900	1370 ±50	1360–1176
2MOST27, w30	pine wood	MKL-5901	1440 ±35	1380–1295
2MOST21B, z20	pine wood	MKL-5902	1110 ±35	1176–1166 (1.5%) 1114–1109 (0.5%) 1073–930 (93.5%)
2MOST21B, w25	pine wood	MKL-4195	1200 ±30	1244–1214 (5%) 1179–1057 (88.3%) 1022–1006 (2.1%)
Single tree trunks				
M1, 6 last tree rings	pine wood	MKL-7158	8890 ±60	10,198–9757
M3, 5 last tree rings	pine wood	MKL-7159	8280 ±40	9426–9128
M30, first 5 tree rings	pine wood	MKL-7173	2785 ±35	2964–2782

The organic deposits were characterized on the basis of microscopic plant tissue analysis using a light microscope (Fig. 4A and Table 2). The peat type was identified according to the Tołpa et al. (1971) classification. The degree of peat decomposition (R) was also determined (Fig. 4A).

POLLEN ANALYSIS

1 cm^3 samples were prepared following the standard procedure described by Berglund and Ralska-Jasiewiczowa (1986). From each 10 cm interval, 16 samples were selected for pollen analysis. Counts were carried out under an *Olympus BX43* light microscope at 600× magnification, with a minimum of 500 terrestrial pollen grains identified per sample. Percentages were calculated based on the sum of arboreal pollen (AP: trees and shrubs) and non-arboreal pollen (NAP: herbaceous and dwarf plants). Pollen diagrams were produced in R Studio (Posit team, 2025) using the *riojaPlot* package (Juggins, 2022). Local Pollen Assemblage Zones (LAPZ) were defined using CONISS cluster analysis (Grimm, 1987; Fig. 5).

Among the non-pollen palynomorphs (NPPs) only *Gelasinospora* was possible to determine.

GEOCHEMISTRY

30 samples, taken every 5 cm, were analysed geochemically. Samples were prepared according to the standard procedure (Pansu and Gautheyrou, 2006). The total content of macro-elements (Ca, Mg, Na, K, Fe) and trace elements (Mn, Cu, Zn, Ni, Pb) were measured using Atomic Absorption Spectrometry (AAS) with *Thermo Scientific iCE 3500* apparatus. Based on content of macro- and micro-elements, several geochemical environmental indicators were calculated: Na/K, Ca/Mg, Na+K+Mg/Ca, Cu/Zn, Fe/Mn, Fe/Ca, and shown on a diagram using Tilia graph software (Grimm, 1991; Fig. 6).

Table 2

Botanical composition, peat type and peat decomposition indicator (R) of the Mosty peatland

Interval [cm]	Peat botanical composition (based on tissues analysis)	Peat type	R [%]
5–10	Peat strongly decomposed; unrecognizable macroremains	Magnocaricioni (sedge peat)	>65
30–35	Peat strongly decomposed; unrecognizable macroremains	Magnocaricioni (sedge peat)	>65
65–70	*Carex gracilis*, *C. pseudocyperus*, *Carex* sp., Musci indet.	Magnocaricioni (sedge peat)	60
90–95	*Carex rostrata*, *Carex riparia*, *Carex pseudocyperus* *Carex* sp. Musci indet.	Magnocaricioni (sedge peat)	60
105–110	*Carex riparia*, Carex rostrata, *Carex pseudocyperus*, *Phragmites australis* *Drepanocladus vernicosus*	Magnocaricioni (sedge peat)	25
120–125	*Dryopteris thelypteris*, *Carex pseudocyperus*, *Carex riparia*, *Carex rostrata*	Magnocaricioni (sedge peat)	50
135–140	*Carex pseudocyperus*, *Carex rostrata*, *Carex gracilis*	Magnocaricioni (sedge peat)	50

Peat type according to the Tołpa et al. (1971) classification; analysis by A. Obidowicz

After drying the samples in a laboratory dryer, they were burned in a muffle furnace at 600°C (6 h), and processed using a PreeKem M6 mineralizer. For each mineralized sample, the concentrations of elements (Ca, Mg, K, Na, Fe, Mn, Ni, Cu, Zn, Pb) were determined by inductively coupled plasma mass spectrometry using an *Agilent 8900 Triple Quadrupole ICP-MS* tandem mass spectrometer (Mass spectrometry branch, Institute of Nuclear Physics, Polish Academy of Sciences, Krakow). Mass interference was reduced by using an interquadrupole collision-reaction cell.

RESULTS

DENDROCHRONOLOGY

SINGLE TREE TRUNKS

The pine trunk ages determined by ^{14}C radiocarbon dating indicates that they entered the sedimentary record at different times. Dendrochronological analysis was performed on the butt of the oldest radiocarbon-dated pine tree, still rooted in the sandy substrate beneath the peat (Fig. 2A: 1 – tree trunk: M2). It was revealed as part of a tree trunk root (~30 cm in diameter) lying nearby (and exposed during excavation), overlain by organic deposits (Fig. 2A: 1 – tree trunk: M1). Tree ring width measurements allowed the development of a dendrochronological curve, averaged for the trunk and its butt section (Fig. 2A: 3). The trunk has 44 tree rings, mostly wide (Fig. 2A: 2). Radiocarbon dating of wood taken from the outer five tree rings of the trunk constrained the date when the pine trunk to ~10,198–9757 cal BP (Fig. 2A: 2, 3).

A second pine tree trunk, also found *in situ* in the lowermost parts of the peat deposits, at the boundary between the peat and the underlying sand, is ~35 cm in diameter (Fig. 2B: 1, 2). Sixty-five tree rings were measured here, and the wood has wide tree rings (Fig. 2B: 3). Wood from the last six tree rings was radiocarbon dated to 9426–9128 cal BP (Fig. 2B: 2, 3).

Another dated pine tree trunk was excavated during exploitation and placed on a spoil heap (Figs. 2C: 1 and 3C). The 10 cm diameter stump showed as many as 152 annual rings, which were remarkably narrow (Fig. 2C: 2, 3). Wood from the first 5 annual rings was radiocarbon dated to 2964–2782 cal yrs BP (Fig. 2C: 2).

FLOATING CHRONOLOGIES

Based on dendrochronological analysis and wiggle matching, two floating chronologies of pine (*Pinus sylvestris*) were developed for the Mosty site (Fig. 3A, B). Their time range is 1360-1187 ±27 mod. cal BP (chronology: 2MOST_A2: 182 years) and 1159–977 ±50 mod. cal BP (chronology: 2MOST_A1 with a length of 172 years) (Fig. 3A, B). Despite the overlapping boundaries of both floating chronologies (1214–1160 mod. cal BP for chronology 2MOST_A2 and 1209–1108 mod. cal BP for 2MOSTA-1 – see Fig. 3A), it was not possible to combine both chronologies into one. This is probably related to the current lack of subfossil tree trunks, analysis of which could allow combining both chronologies. Averaged dendrochronological curves for both chronologies indicate periodic, longer reductions in tree ring widths in the years ca: 1320–1298, 1268–1258; 1224–1210 cal BP and (for the younger chronology): 1128–1118; 1064–103; 994–982 cal BP (Fig. 3A: 2, B: 2). More frequent are short-term reductions in growth (lasting 4–8 years), which may indicate brief deteriorations of ecological conditions in the habitats of these trees (Fig. 3A: 1, B: 1).

AGE-DEPTH MODEL AND SEDIMENTARY RATE

The age-depth model constructed shows a high agreement index (Amodel: 82%), indicating that the chronology is reliable (Fig. 4B; Bronk Ramsey, 2009, 2017). The modelled age developed based on the age-depth model for each 0.5 cm interval of the profile have been shown as mod. cal BP.

According to the model, the sedimentary accumulation rate varied from 0.05 to 0.42 mm yr^{-1} (0.24 mm yr^{-1} on average). Maximum AR values (3.2–4.2 mm yr^{-1}) occurred during the deposition of sedge peat, while minimum AR values (0.05–0.06 mm yr^{-1}) corresponded to the accumulation of organic muds and strongly decomposed peats.

SEDIMENTARY SEQUENCE

Drilling with the INSTORF bit reached a depth of 167 cm, penetrating the sands underlying the organic deposits (Fig. 4A,

D). These sands have been OSL dated to 22.9 ±3.4 ka BP (UJK-OSL-101) (Fig. 4A).

The beginning of accumulation of highly contaminated peat (60% loss on ignition) at a depth of 154 cm was dated to 9258 ±130 mod. cal BP. The increase in organic content (90% loss on ignition) and accumulation of uncontaminated peat at a depth of 140 cm was dated to 9393 ±100 mod. cal BP (Fig. 4A, D). The organic deposits are dominated by sedge peat (genus: *Magnocaricioni*, according to Tołpa et al., 1971). In the 154–120 cm interval this is formed by sedges: tissues of *Carex rostrata, C. gracilis, C. riparia, C. pseudocyperus*, and the fern *Dryopteris thelypteris*, were identified; the degree of decomposition was 50%, and loss on ignition reached 90% (Fig. 4D and Table 2). The peat accumulation rate here is 0.35 mm yr^{-1} (Fig. 3B). In the 120–110 cm interval, the sedge peat is less decomposed (R = 25%, loss on ignition: 90%), and the sedges are accompanied by *Phragmites australis* and *Drepanocladus vernicosus* moss. Towards the top of the profile, the degree of decomposition of the sedge peat (formed here exclusively from sedges) increases to 60% (105–65 cm; LOI: 80%). In the 110–105 cm interval, the loss on ignition curve shows a decrease in loss on ignition from 90 to 45%. This episode was dated to 8459–8200 ±74 mod. cal BP (Fig. 4A, C). On the profile shown on a time scale, the decrease in loss on ignition appears to be very short-lived (Fig. 4C). The second decrease in loss on ignition values, visible on the LOI curve in the 60–52 cm interval, is longer. This episode was dated to 7348–6283 ±120 mod. cal BP (Fig. 4A, C). In the highest parts of the sedimentary profile (35–0.0 cm), the peat is already highly decomposed (humified) (R >65%) and mineralised, and plant tissues are undetectable. The sediment accumulation rate decreases here to 0.05 mm yr^{-1}(Fig. 4A, B). From a depth of 25 cm, a steady decrease in loss on ignition to 35% is visible, while the peat accumulation rate increases to 0.3 mm yr^{-1} (Fig. 4B). The onset of this process has been dated to 1522 ±140 mod. cal BP and has continued to the present day (Fig. 4A, C). Its onset also coincides with the temporal range of the pine chronologies (Fig. 4A, C).

VEGETATION HISTORY

The Mosty pollen record spans most of the Holocene and was divided into five distinct LPAZ, with one interval lacking pollen, as identified in the sequence (Fig. 5).

During the earliest phase (LPAZ MO-1, before 9524–8468 cal BP), the record indicates a clear dominance of *Pinus*. *Picea* also played a role more substantial than that of a short-lived incursion in the local vegetation, while temperate deciduous taxa, including riparian species, were rare. The increase in *Poaceae* pollen at the end of the zone suggests local forest contraction. The presence of *Filicales monolete* spores and Cyperaceae pollen might suggest the expansion of sedge fen. A sample at 105 cm depth contains no pollen, likely reflecting sedimentary conditions unfavourable for palynomorph preservation ~8468–8201 cal BP (Fig. 5).

In the subsequent phase (LPAZ MO-2, 8201–7718.5 cal BP), *Pinus* declined synchronously with an expansion of *Picea* and *Alnus*. Other temperate taxa remained of minor importance. In this zone, *Gelasionsopora* spores were observed (Fig. 5).

In LPAZ MO-3 (7718.5–6872.5 cal BP), *Pinus* regained dominance, while *Alnus* disappeared completely from the record. This phase also records the maximum expansion of *Corylus*, which played a prominent role in the forest vegetation at this time.

The vegetation of LPAZ MO-4 (6872.5–3647.5 cal BP) is characterized by moderate changes. *Pinus* remained dominant, but both *Picea* and *Alnus* regained importance, though less than in earlier phases.

The final zone (LPAZ MO-5, 3647.5 cal BP) reflects the vegetation dynamics of the Subboreal and Subatlantic periods. *Pinus* continued to dominate, while *Fagus* and *Abies* appeared in the record but remained scarce. Increases in non-Arboreal pollen, particularly Poaceae, Amaranthaceae and *Artemisia*, indicate forest contractions, most likely driven by human activity. No other strong indicators of anthropogenic impact are present (Fig. 5).

Overall, the Mosty pollen sequence represents an unusually well-preserved record dominated by *Pinus*. A striking feature is the intermittent representation of taxa such as *Alnus, Betula, Corylus,* and *Quercus*, as well as the underrepresentation of riparian taxa. The complete absence of *Fraxinus* pollen is particularly unusual given the site's location in a river valley.

GEOCHEMICAL INDICATORS

Based on variations in organic matter content (LOI) and the concentrations of macro- and trace elements, four main geochemical zones were determined: GZ I–IV (Fig. 6).

The first geochemical zone (G 1; 150–110 cm; before ~9520 to ~8460 mod. cal BP), coinciding with the transition between coarse sands and sedge peat, is divided into two subzones: G 1A and B. The older stage (G1 A, before 9390 mod. cal BP), associated with the deposition of coarse sands with a gradually increasing content of organic matter (LOI: 0.9–25%), is characterized by elevated concentrations of K (0.68–1.27 mg/g) and Mg (0.85–1.31 mg/g). Elevated values of the basin erosion ratio (Na+K+Mg/Ca) were accompanied by values, lower than the profile average, of the Fe/Mn ratio, indicating the dominance of oxidizing conditions. The upper part of this zone (G1 B; 9390–8460 mod. cal BP) is associated with accumulation of sedge peat. During this stage of peatland development, the content of organic matter increases distinctly (from 45.8 to 90.3%) as does the concentration of calcium (1.6–24.4 mg/g) and some trace elements: Ni (from 0.51 to 14.6 µg/g) and Cu (from 3.2 to 13.8 µg/g). Decreasing redox conditions, reflected in the highest Fe/Mn ratios within the entire sedimentary sequence (108–131) and accompanied by a declining content of lithophile elements (Na, Mg, K), indicate a rise in the groundwater level in the peatland, without evidence for the deposition of river-derived allochthonous clastic material (Fig. 6).

The onset of the next geochemical zone (G 2; 110–60 cm; ~8460–7200 cal BP) is marked by the deposition of a thin layer (<10 cm) of silty peat (LOI: 75.5–50.9%). Elevated values of indicators associated with mechanical erosion (Na+K+Mg/Ca, Fe/Ca), together with a substantial increase in trace elements such as Zn and Pb (up to 68.5 and 52.4 µg/g, respectively), can be interpreted as reflecting the deposition of overbank sediments during flood events of the Biała Nida River. After ~8150 cal BP an increasing content of organic matter delineates the beginning of the sub-zone G2 B (Fig. 6). In this stage, the concentrations of most macroelements (Ca, Mg, Fe, K) returned to levels comparable to those observed prior to the clastic influx (Fig. 6). In contrast, the mean sodium concentration was approximately three times higher (µ = 0.58 mg/g) compared to the

preceding sedge peat horizon (μ = 0.18 mg/g), resulting in a significant increase in the Na/K ratio. These geochemical characteristics, together with stable and extremely low values of the erosion ratio (μ = 0.11) and overall low Fe/Mn values (μ = 118.1), may indicate a lowering of the groundwater level in the peatland (Fig. 6B).

The beginning of the next geochemical zone (G3; 60–30 cm; ~7200–1770 mod. cal BP) is characterized by a significant decrease in organic matter content (from 81 to 65%), associated with another peat horizon enriched in overbank deposits. The rapid decrease in the accumulation rate (from 0.33 to 0.05 mm yr^{-1}) during the deposition of this interval may indicate the presence of a hiatus or hiatuses. Increasing concentrations of lithophile elements, as well as flood-delivered trace elements from the Nida River catchment (Zn, Pb), were recorded ~6283 mod. cal BP (Fig. 6A).

The uppermost geochemical zone (GZ IV; 30–0 cm; ~1770 to –79 cal BP) consists of strongly humified peat (see Figs. 4A and 6A). The concentrations of elements, except for Ca, increase upwards, reaching their highest values in the entire sedimentary sequence. The distinct increase in trace elements such as Pb and Zn (86.1 and 135.7 μg/g, respectively) during this phase, in contrast to the earlier flood-related peaks of Pb and Zn, is interpreted as resulting from atmospheric deposition and their accumulation within the zone of water-level fluctuation (Damman, 1978).

DISCUSSION

PALAEOENVIRONMENTAL RECORDS IN PEATLAND DEPOSITS

Previous research indicates that the sands underlying the Mosty peatland deposits were originally fluvioglacial, related to the disappearance of the Odranian ice sheet (Saalian) (Hakenberg, 1974). Later, they were reworked by denudation and fluvial processes during the Eemian Interglacial and in the Vistulian Glacial (Hakenberg, 1974; Dzierżek et al., 2019). The alluvial floodplains of the Czarna and Biała Nida rivers and their interfluve areas are dominated by Pleistocene braided river sands forming an alluvial terrace (Kalicki and Biesaga, 2024).

The OSL date of 22.9 ±3.4 ka BP we obtained from the sands directly underlying the peat indicates that the last exposure of these deposits took place at the end of the Younger Plenivistulian (Fig. 4A). This exposure was undoubtedly related to the reworking of fluvioglacial sands by the fluvial activity of the Biała Nida and the Czarna Nida rivers in the Upper Plenivistulian, as indicated by the date (see Krupa, 2013, 2015; Kalicki and Biesaga, 2024; Fig. 4D). The luminescence date of 19.18 ±2.88 ka BP (Krupa, 2013), very close to that obtained by us, determines the age of the sandy alluvia of the Czarna Nida River, also in Mosty (Mosty 1, see on Fig. 1C – site 1; Krupa, 2013, 2015).

The onset of sedge peat accumulation in the Mosty peatland (this study), formed by paludification of a cut-off meander, was radiocarbon dated to ~9543–9196 cal BP (9258 ±130 mod. cal BP; Fig. 4A and Table 1). The significant age difference between the sandy deposits (Upper Plenivistulian) and the onset of peat accumulation (Boreal phase of the Holocene) indicates the occurrence of a hiatus at this level, resulting from erosional removal of the upper part of the sand unit. At the beginning of the Late Glacial (~17,900–17,400 cal BP), a stage of channel incision into the substrate was recorded in the valley of the neighbouring Czarna Nida River, associated with increased river erosion (Krupa, 2013; Kalicki and Biesaga, 2024). The formation of large meanders in the Czarna Nida valley has taken place at least since the interphase warming of the Allerød (~13.9 ka cal BP; Krupa, 2013; Kalicki and Biesaga, 2024). Later, after the formation of braided channels during the cooling of the Younger Dryas (~12.7 ka cal BP), already at the beginning of the Holocene (11.6 ka cal BP) and in the Eo- and Neoholocene, a constant tendency of the Czarna and Biała Nida rivers to cut into the substrate and to form meanders was observed (Krupa, 2013, 2015; Kalicki and Biesaga, 2024).

Similar trends at that exact time have been widely observed among European river valleys (Vanderberghe et al., 1994; Panin et al., 1999), including the Vistula River valley (Starkel et al., 1996, 2013; Kalicki, 2006). At that time, erosion likely removed the upper parts of Vistulian deposits, i.e., the sandy alluvial succession of the Biała Nida that underlay the Mosty peatland. At the mouths of the Biała and Czarna Nida rivers, a floodplain began to form in the Eoholocene, following the dissection of a higher river terrace (and the formation of meanders) that had previously formed in the Younger Dryas, when the river was still of braided type (Krupa, 2013). During the Eoholocene, particularly in the Preboreal phase, a gradual calming of fluvial processes was observed in the Biała and Czarna Nida River valleys (Krupa, 2013; Kalicki and Biesaga, 2024). The subsequent expansion of pine-birch-spruce forests (Fig. 5) limited the supply of material to the river channels. River meanders were then cut off and paludified, as shown by the onset of organic accumulation in cut-off palaeomeanedrs dated in the Czarna Nida valley to 11,204–10,793 cal BP (Kuby Młyny palaeomender – for location see Fig. 1B) and 9401–8722 cal BP (Mała Wieś oxbow lake) (Krupa, 2013). In the Biała Nida River valley, the meander cut-off in Mosty-Browica (above the Mosty site analysed) and its paludification occurred ~9393–8649 cal BP (Fig. 1C – site 4) (Kalicki and Biesaga, 2024). During this period, the Biała Nida meander in Mosty was also cut off (this study) and paludification gradually began (Fig. 1B – research site).

The oldest pine trunk found in the deposits of the Mosty site, the butt part of which is still rooted in the sandy substrate, has been radiocarbon dated to 10,198–9757 cal BP. The date obtained from the wood of its last 5 tree rings indicates the time when it fell (Fig. 2A). Despite the relatively large trunk diameter (30 cm), the tree has only 44 tree rings, which are generally wide. However, the two-fold reduction in annual tree rings visible on the curve in the first 6 years and around the 25th–30th year of tree growth may indicate a rapid deterioration of ecological conditions, perhaps related to periodic flooding of the habitat. Another, slightly younger pine trunk found in the bottom parts of the peatland had fallen ~9426–9128 cal BP (here, wood from the last 5 growth rings were also dated) (Fig. 2B and Table 1). Compared to the previous trunk, it has wider rings: with a diameter of 35 cm, it has 67 annual rings (Fig. 2B: 3). The dated onset of peat accumulation indicates that the older pine (M1/M2) grew on sandy substrate, prior to the formation and onset of paludification of the Biała Nida palaeomeander, within a riparian forest covering the Biała Nida River floodplain. This woodland phase was possible at that time, as a distinct decline of fluvial activity and peat formation was observed in Central Europe, including the Vistula River, ~10,200–9600 cal BP (Starkel et al., 2013). The younger subfossil pine stump (M3: 67 year old – see Fig. 2B: 3) fell in ~9426–9128 cal BP, and also grew partly on sandy substrate (the tree trunk was contaminated by sand). The width of its annual rings also indicates that it was (to a lesser extent) subjected to fluvial processes, also being part of the riparian forest formed at the beginning of meander paludification (Fig. 7A). The time when it fell coincided with a distinct rise in fluvial activity of European rivers, estimated

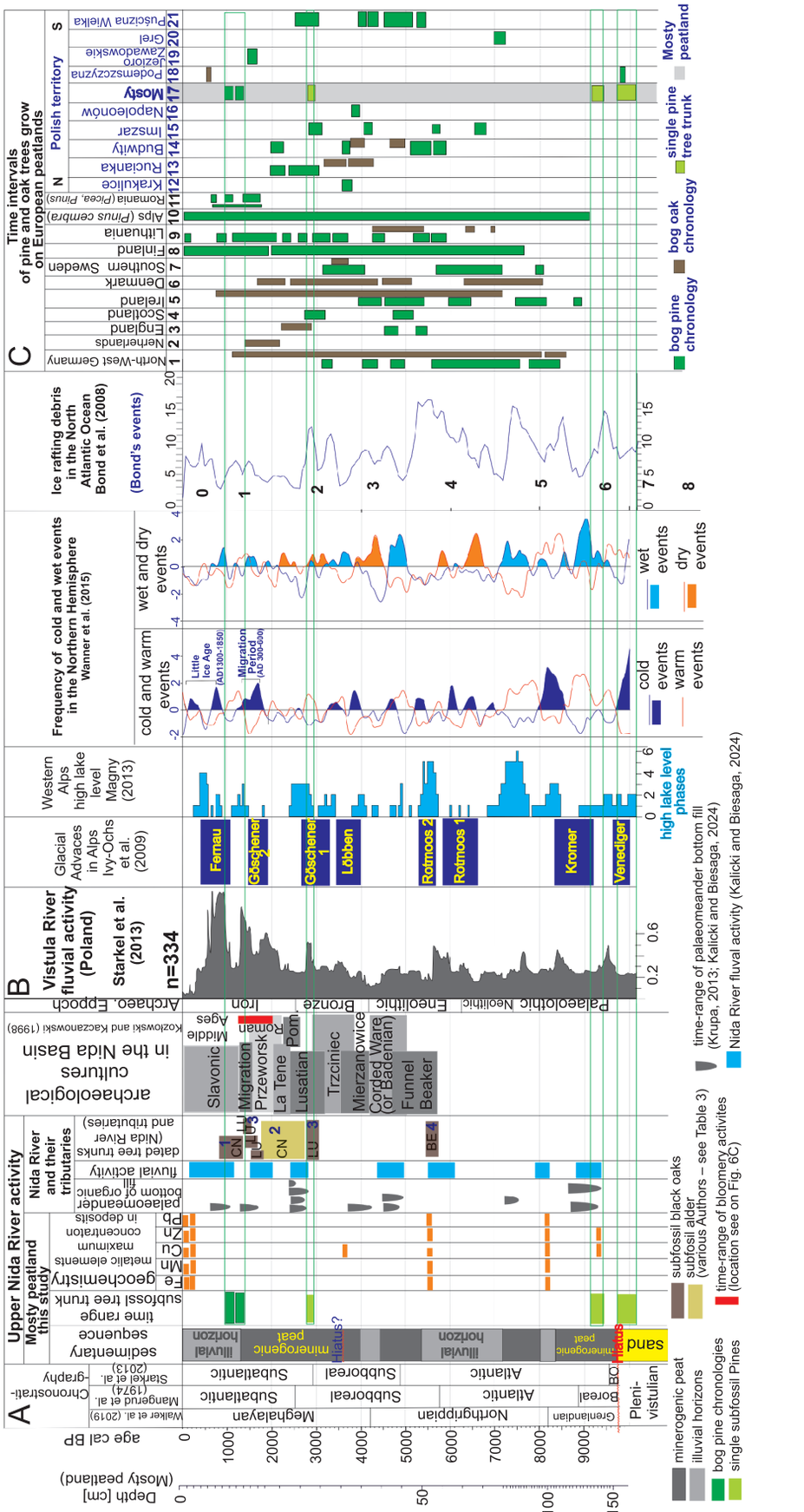

Fig. 7. Time range of subfossil pines (single and floating chronologies) *versus*: A – local palaeoenvironmental changes recorded in the Mosty peatland: start of abandoned palaeomeander fills by organic deposits in the upper Nida and their tributaries, and Nida River fluvial activity: after Krupa, 2013; Kalicki and Biesaga, 2024; subfossil trees in Upper Nida and their tributaries: CN – Czarna Nida River; LU – Lubrzanka River; BE – Belnianka River: (see Table 3 – site location according to current numbers – on Fig. 1B); B – common palaeoclimatic changes recorded in the Northern Hemisphere (after various authors); C – correlation of subfossil bog pine and bog oak chronologies in European and Polish peatlands

The Mosty peatland (site 17) is marked in grey; the location and authors of all chronologies are shown in Figure 8 and Table 3, according to the site numbers

at ~9600–8400 cal BP (Starkel et al., 2013). In the Northern Hemisphere, a strong increase in climate humidity occurred at that time (Wanner et al., 2015), as well as the strong cooling resulting in a Bond event ~9.4 ka (Bond et al., 2008) and the Venediger phase of the Glacial advances in the Alps (Ivy-Ochs et al., 2009; Le Roy et al., 2024; Fig. 7B). A phase of increased fluvial activity of the Wisła River was also recorded at that time (Starkel et al., 1996, 2013; Fig. 7B). Undoubtedly, when the younger pines fell coincided with the beginning of paludification of the Biała Nida abandoned meander studied in Mosty. The palynological diagram is dominated by *Pinus sylvestris* with the participation of *Betula* and *Picea* and a small share of *Corylus* pollen (Fig. 5).

The delivery of clastic sediments to the Mosty peatland and the formation of the illuvial horizon in the peats (probably an effect of the Biała Nida flooding), visible on the LOI curve, was dated to 8459–8200 ±72 mod. cal BP (Fig. 4A, C). At this time, pollen is absent on the palynological diagram (Fig. 5). During this interval, a sudden increase in the content of Mg and K, as well as the heavy metals Fe, Mn, Ni, Cu, Zn, and Pb, supplied by the floodwaters of the Biała Nida River (and especially its tributaries – the Wierna Rzeka and Hutka rivers – see location on Fig. 1B) is visible (Figs. 6A and 7A). The source of these elements in the Holocene deposits of Biała Nida was undoubtedly polymetallic mineralization in the Devonian limestones of the Miedzianka Mt. region, which is directly drained by tributaries of the Hutka River, a left tributary of the Biała Nida River (see Fig. 1B). The primary mineralization at Mt. Miedzianka is polymetallic, the predominant minerals here being sulphides of copper and iron (chalcopyrite), lead (galena), copper, arsenic, nickel, barium and antimony, with the presence of silver and zinc in the crystal lattices of these minerals (Rubinowski, 1971; Pabian et al., 2022). However, the deposit of economic importance was the secondary, karst-weathering accumulation of sulphide, carbonate and oxide copper minerals, as well as copper and iron with admixtures of native silver and native copper in clay-sandy deposits, which filled mainly karst voids located high on the slopes of the hills. Generally, the deposit (formerly mined) shows elevated contents of Cu, Pb, Zn, As and Fe, and slightly lower, but reaching several percent, values in certain minerals of Ti, Ni, Sb, Mo, Ag, and Ba (Rubinowski, 1971; Swęd et al., 2015). The presence of this deposit on the relatively steep slopes of Miedzianka Mt., several tens of metres high (354 m a.s.l.), resulted in increased mineral supply to streams during intensified denudation processes, stimulated, for example, by increased climate humidity. Therefore, during the period analysed, there would have been natural delivery of these elements to the Hutka River (and later the Biała Nida River) alluvium.

These elements were therefore delivered to the Mosty peatland by floodwaters of the Biała Nida River. Flooding of the peatland at this time is indicated by a substantial increase in the Fe/Mn ratio in this part of the succession, indicating an increase in the water level in the peatland (Fig. 6B; Davison, 1993; Mazurek et al., 2014; Borówka et al., 2015). These flooding events (8460–8250 cal BP) coincide with the most prominent Holocene climate deterioration, the so-called 8.2 ka event (*sensu* Bond et al., 1997, 2008). Minor changes in the accumulation rate of sedge peat in the sedimentary profile studied (μ = 0.31–0.42 mm yr^{-1}) during this climate event (Fig. 4B) may indicate slow floodplain deposition, presumably resulting from the considerable distance of the peatland from the river channel, and/or low-magnitude, cyclic flooding events (Knighton, 1998; Hupp, 2000). The flooding of the peatland by the Biała Nida River and the deposition of the illuvial horizon in the peats coincided with one of the largest and most rapid climate cooling and humidity growth events in the Holocene: the famous 8.2 ka event (Bond et al., 2008; Wanner et al., 2011, 2015; Walker et al., 2019; Fig. 7B). At that time, an increase in fluvial activity of European rivers was recorded, especially the Wisła River (Fig. 7B; Starkel et al., 1996, 2013), and an intensification of slope processes in mountain areas (Pánek et al., 2013; Margielewski, 2018). In the Alps, this cooling was reflected as the Kromer phase of the glacial advances (Ivy-Ochs et al., 2009; Le Roy et al., 2024; Fig. 7B). In the valley of the neighbouring Czarna Nida River and their tributaries, in the older part of the Atlantic phase, traces of individual floods were recorded in alluvium, in the form of peat being overlain by clastic sediments in several oxbow lakes (Ludwikowska-Kędzia, 2000; Krupa, 2013, 2015). At that time, in the valleys of the Czarna and Biała Nida rivers, the river meanders were cut off and their paludification began (Fig. 7A; Krupa, 2013; Kalicki and Biesaga, 2024).

In the profile of the Mosty peatland analysed, the beginning of further supply of clastic sediment to the mire was dated to 7348 ±87 mod. cal BP, while the end of this long-term process, which formed the illuvial horizon in the peats, was dated to 5827 ±87 mod. cal BP (Fig. 4A, C). In the light of the dating, this process lasted almost 1500 years and was permanent: the LOI curve does not show the fluctuations characteristic of frequently repeated events (Fig. 4A, C). The palynological diagram shows a decrease in the share of *Pinus* pollen, with a simultaneous increase in the share of *Betula*, *Picea*, *Ulmus*, *Alnus* and *Corylus* pollen. Poaceae and Cyperaceae also appear (Fig. 5). The elemental composition of the sedimentary interval analysed shows a sudden increase in the contents of Fe, Mn, Cu, Zn, and especially Pb, as well as an increase in the share of Mg and K (Figs. 6A and 7A), delivered to the peatland by floodwaters of the Biała Nida River and the Hutka River flowing into it. The increase in the Fe/Mn ratio indicates periodic flooding of the peatland with water (Fig. 6B). Increasing concentrations of lithophile elements, as well as flood-delivered trace elements from the Biała Nida and Hutka rivers catchment (Zn, Pb), may indicate a link with the cold and wet climate excursion (6500–5900 cal BP) documented at a large number of study sites across Europe (Wanner et al., 2011, 2015; Florescu et al., 2019; Kołaczek et al., 2021). Around 5.9 ka BP, an episode of significant climate cooling called a Bond event was recorded (Bond et al., 2008; Fig. 7B). In the Alps, the Rotmoos 1 phase of mountain glacier advances occurred (Ivy-Ochs et al., 2009). Around 6400 cal BP a distinct increase in peat growth and fluvial activity was recorded in central Europe, including the Wisła River Valley (Starkel, 2013; Fig. 7B). In the cut-off oxbow lakes of the Nida River, peats began to accumulate, dated in the Biała Nida palaeomeander to 6724–6313 cal BP (Fig. 1B – site 4 and Fig. 7A; Kalicki and Biesaga, 2024), and similarly to the Mosty peatland analysed, these were mainly clayey peats (ash content ~50%).

A series of small mineral sediment intercalations into the Mosty peatland (poorly marked on the LOI curve in the 45–32.5 cm interval) indicating local inundation of the peatland (floods?), which could have occurred ~4460–2178 ±200 mod. cal BP (45–32.5 cm; Fig. 4A, C). In the deposits, an increase in Cu content is visible (lower parts of the interval), while towards the top of this interval a slight increase in Fe and Mn was recorded, with a decrease in the concentration of other heavy metals (Figs. 6A and 7A). A slight increase in the Fe/Mn ratio in this interval may suggest local, small flooding (floods?) of the Mosty peatland (Fig. 6B). With the beginning of the “flood period” ~4460 cal BP recorded in the Mosty peatland deposits, the cutting off and paludification of the Czarna Nida palaeomeanders began (Krupa, 2013; Fig. 7A). The fluvial activity in the Czarna Nida interfluvial area at that time may be indicated by the cut-off and the beginning of paludification of the Czarna Nida mean-

ders in Mosty (4233–3724 cal BP – see Fig. 1C – site 2) and in Borki (4961–4531 cal BP – see Fig. 1C – site 3 and Fig. 7A; Krupa, 2013; Kalicki and Biesaga, 2024).

However, the low accumulation rate in the Mosty peatland (AR) (0.5 mm yr^{-1}) may, in turn, suggest a slowdown in the rate of peat accretion due to periodic drying of the peatland (Fig. 4B). The sequence of radiocarbon dates, the rapid decrease in the peat accumulation rate, the collapse of the age-depth curve, and the occurrence of extremely decomposed peats (R >65%) at this level, typical of peatland desiccation, indicate the possibility of a hiatus occurring here (in the interval between 45–30 cm, although peat compaction could also have occurred here; Fig. 4A, B). However, at the current level of research, its temporal extent is difficult to determine, because of a shortage of radiocarbon dates, and it is also not confirmed by palynological analysis (see Fig. 5). It cannot be ruled out that the peatland desiccation (resulting in the lack of peat sedimentation) could have been related to the 4.2 ka episode, during which climate cooling and simultaneous desiccation occurred in this part of Europe (Wanner et al., 2011, 2015; Kaniewski et al., 2018; McCay et al., 2024; see on Fig. 7B).

In the areas adjacent to the Biała Nida River valley, pine forest (*Pinus sylvestris*) still dominated at that time, though with a clear decrease in the share of pine and with a significant admixture of spruce (*Picea abies*), birch (*Betula*) and alder (*Alnus*; Fig. 5).

In the upper parts of this interval (~35 cm) there was a pine trunk characterized by very narrow tree rings (Fig. 2C). The beginning of its growth (first 5 tree rings) was radiocarbon dated to 2964–2782 cal BP, while the tree fell in ~2815–2632 cal BP (taking into account its 150 annual rings) (Fig. 2C: 2, 3). Dendrochronological analysis showed that the tree grew in ecological conditions that suddenly deteriorated dramatically during the tree's growth. While the first 7 tree rings are 180 μm wide, over time their width drastically decreases: after 20 years to 65–40 μm, and after another 70 years of tree growth (~2,894–2,712 cal BP), the width of the annual increments decreases to 10–20 μm (Fig. 2C: 3 – compare with tree ring curves: A3 and B3 in Fig. 2). The tree likely grew on the surface of a peatland (bog pine) that was initially extremely dry (tree germination phase) but quickly became subject to frequent rising water levels due to long-term flooding of the Biała Nida River, which resulted in a dramatic reduction in the width of the tree's annual rings. The tree's falling may have been related to climate deterioration ~2.8 ka (Bond event), when increased fluvial activity of the Wisła River was recorded (Starkel et al., 2013), coevally with the advance of the Alpine glaciers during the Goeschener phase (Ivy-Ochs et al., 2009), and high water levels in Alpine lakes (Magny et al., 2003; Magny, 2013; Fig. 7B).

At the end of the Subboreal and early Subatlantic phases, an erosional stage began in the Czarna Nida valley (Krupa, 2013, 2015; Kalicki and Biesaga, 2024). In the period 2.8–2.4 ka cal BP, the cutoff of meanders and the beginnings of their paludification are common (Krupa, 2013; Fig. 7A). The meandering channels of the Nida River and its tributaries migrated laterally at that time, as indicated by a fallen black oak (*Quercus*) tree trunk found in the alluvial deposits of one of the Czarna Nida tributaries (Lubrzanka – see Fig. 1B), dated to 3061–2783 cal BP (Kowalski, 2002). A subfossil alder (*Alnus*) tree trunk dated to 2725–1742 cal BP found in the Czarna Nida alluvial deposits at Borki (Fig. 1B – site 3 and Table 3; Śnieszko, 1978; Krupa, 2013), has also been associated with this erosion phase. This tree trunk could have fallen during the same wet phase as the trunk with thin annual tree rings from the peatland analysed in Mosty (this study – Fig. 2C).

Although the Czarna Nida erosional stage began at the turn of the Subboreal and Subatlantic phases, the greatest concentration of this type of erosion-related event was recorded in the Roman period (Krupa, 2013; Kalicki and Biesaga, 2024). The area between the Biała and Czarna Nida rivers was then included in the Nida iron smelting region (with famous bloomeries) of the Przeworsk Culture (Fig. 6C). The activity of this bloomery smelting centre in the Czarna and Biała Nida valleys took place in the years from 2316–1929 cal BP (366 BC–21 AD), to 1529–1299 cal BP (421–651 AD) (Przychodni, 2006; Przepióra et al., 2024; Kalicki and Biesaga, 2024). Traces of smelting and iron processing activities are macro- and micro-slags and iron pellets (so-called spherules) from this period, found in the alluvial deposits of the Biała and Czarna Nida rivers, in the interfluve zone (Fig. 1B – sites 6 and 7; Kalicki et al., 2020; Przepióra et al., 2023; Kalicki and Biesaga, 2024). In-

Table 3

Dated subfossil tree trunk excavated from the Mosty peatland (Biała Nida River; this study) and the Czarna Nida River, and their tributaries: the Lubrzanka River and Belnianka River (site location on Fig. 1B)

River	Site	Wood species	Age cal BP	Age BC/AD	Source
Biała Nida	Mosty M1	Pine	10,198–9757		this study
	Mosty M3	Pine	9426–9128		
	Mosty M30	Pine	2964–2782		
	Mosty, floating chronology 2MOST_A2	Pine	1360–1187 ±27 mod.cal BP		
	Mosty, floating chronology 2MOST_A1	Pine	1158–976 ±50 mod. cal BP		
Czarna Nida	Borki	Alder	2725–1742	775 BC–209 AD	Śnieszko (1978); Krupa (2013)
	Wolica	Oak	1341–804	609–1146 AD	Lindner (1977)
Lubrzanka	Cedzyna	Oak	3061–2783	1111–833 BC	Kowalski (2002)
	Cedzyna 2	Oak	1828–1570	125–380 AD	Kowalski and Swałdek (1991)
	Cedzyna 1	Oak	1694–1404	256–546 AD	
	Cedzyna 1	Oak	1517–1305	433–645 AD	
Belnianka	Czaplów	?	5741–5482	3791–3532 BC	Ludwikowska-Kędzia (2000)

terestingly, the period of this economic activity did not significantly figure on the geochemical diagram of the Mosty peatland deposits. Only a local increase in the Fe, Mn, Cu and Zn contents is visible (Fig. 6A). The development of the bloomery activity in the interfluve of the Biała Nida and Czarna Nida rivers (see Fig. 6C) and intensive environmental transformations in the "industrial" part of the river basin coincided with a period of more frequent occurrence of extreme hydrometeorological phenomena (Kalicki, 2006; Starkel et al., 2013). This resulted in the intensification of fluvial processes in the area analysed, lateral migration of channels (so-called black oaks in the alluvium of the Nida and its tributaries – see Fig. 7A and Table 3), and the formation of new alluvial intercalations with residues of sediments from metallurgy and iron processing. Deforestation related to the production of charcoal used in the metallurgical process resulted in the activation of aeolian processes in the interfluve area ~2336–1415 cal BP (Borki site – see Fig. 1B:–site 3; Krupa, 2013; Kalicki and Biesaga, 2024).

The top of the Mosty peat succession, in the 0–25 cm interval, is dominated by strongly decomposed (R >65%) and highly clayey peats (Table 2), resulting from a long-term supply of clastic sediment to the peatland (LOI decreases from 80–35%). Its onset was dated to 1522 ±148 mod. cal BP (428 cal AD; Fig. 4A, C). Hypothetically, it can be assumed that this significant reduction in loss on ignition could also be the result of mineralization of the top parts of the peat, as frequently occurs in the peat profiles described (Borówka et al., 2015). However, at least several observations indicate otherwise. The onset of illuvial horizon formation coincided with a period of widespread climate wetting and cooling in the 5th–6th century AD (Kalicki, 2006). At that time, both an increase in the fluvial activity of the Wisła River (Starkel et al., 1996, 2013) and a phase (Goeschener 2) of glacial advance in the Alps (Ivy-Ochs et al., 2009) were recorded (Fig. 7B). With the beginning of the formation of the illuvial horizon in the top part of the organic deposits of the Mosty peatland (so-called clayey peats), the common falling of pine trunks and their accumulation in the sediment occurred (Fig. 4A, C). The floating chronologies compiled on their basis have a time range of 1360–1187 ±27 mod. cal BP (590–763 ±27 mod. cal AD) and 1158–976 ±50 mod. cal BP (792–974 ±50 mod. cal AD) (Fig. 2A, B). The dying-off phases of trees found here indicate several episodes of tree falling, dated 1201–1187 ±27 mod. cal BP (749–763 ±27 mod. cal AD) and 1002–976 ±50 mod. cal BP (Fig. 2A, B). Hypothetically, this may indicate that, in these periods, lateral migration of the Biała Nida River could have taken place, which caused undercutting of the forested river banks, the falling of trunks of the pine trees growing there, and their deposition in the form of driftwood. Similar phenomena have been described for subfossil oaks (so-called black oaks) from the alluvia of the lower Wisła (Kalicki and Krąpiec, 1995). However, the paludification involved an abandoned meander, not an active meander, and the supply of clastic sediment into the peatland by flood waters was quite moderate. Clastic sediments delivered by periodic floods did not interrupt peat accumulation, and sedimentation of clastic layers (even thin ones) typical of floods did not occur here (see Klimek, 1974; Teisseyre, 1988). The river's fluvial activity was evident only in the form of a relatively small (albeit permanent, lasting for at least 1500 years) supply of clastic sediment to the peatland and the formation of an illuvial horizon in the peat. The relatively low content of clastic sediment delivered to the peatland by river waters indicates that the river current during floods was not sufficiently powerful to move the numerous tree trunks and deposit them within the peatland sediments.

The floating chronologies of the pines as compiled (with several germination and dying-off phases) cover the 6th–8th centuries and the 8th–9th centuries AD (Fig. 3A, B). The beginning of these chronologies is therefore coeval with the beginning of the spread of Slavonic colonization since the 6th century in the European areas (after depopulation during the Migration Period 375–550 AD – see Fig. 7A). This colonization phase was also noted in the interfluve of the Biała and Czarna Nida rivers (Fig. 6C; Kozłowski and Kaczanowski, 1998). The pine falling phase coincided with a significant increase in climate humidity in the 5th and 6th century with several fluctuations, which is corroborated by several dying-off tree phases of this chronology. After the Migration Period, pollen diagrams record a sudden increase in anthropopressure in the Nida valley (NAP increase above 50%; Szczepanek, 1961, 1982), although in the Mosty profile this process was less pronounced (Fig. 5). Typically, such element concentrations in the top layers of peatland sediments are associated with atmospheric deposition (Pawełczyk et al., 2018). However, in this case, the higher element concentrations compared to the earlier illuvial levels could have been more complex and originated both from atmospheric deposition and from the delivery of waste from the smelting activity to the alluvia (see Kalicki and Biesaga, 2024) or from mining activities at Miedzianka Mt. (Rubinowski, 1971).

ORIGIN OF SUBFOSSIL TREE TRUNK IN THE LIGHT OF DENDROCHRONOLOGY: DRIFTWOOD, RIPARIAN FOREST OR BOG PINE WOODLAND

So far, the origin of all subfossil tree trunks in the deposits of the Nida River or its tributaries (Czarna Nida and its tributaries: Lubrzanka and Bielnianka rivers) has been associated with the lateral migration of river channels (meanders) during the phase of increased erosion. This was justified because most of these tree trunks (black oaks, alder) were embedded in alluvial sediments (sands, silts; Fig. 7A and Table 3; Lindner, 1977; Kowalski and Swałdek, 1991; Ludwikowska-Kędzia, 2000; Kowalski, 2002; Krupa, 2013; Kalicki and Biesaga, 2024). However, the pine trunks at the Mosty site are buried in the organic deposits of a fluviogenic peatland formed as a result of paludification of an abandoned meander of the Biała Nida River (Figs. 2, 3 and 7A). Therefore, an important issue for the reconstruction of palaeoenvironmental changes in the interfluve of the Biała and Czarna Nida rivers is to explain the origin of this wood in the peat deposits.

A subfossil trunk of the oldest pine tree (*Pinus sylvestris*) found in the Mosty peatland has preserved its butt end, still rooted in the sandy substrate (Fig. 2A: 1), its fall dated to 10,198–9757 cal BP (Fig. 2A). This pine grew on sandy substrate, before the onset of paludification of the Biała Nida palaeomeander and it is likely a remnant of pine woodland that then covered the Biała Nida River floodplain. The wide annual growth rings indicate generally favourable growing conditions for the tree. During the period in which the tree was growing, neither cooling nor humidification of the climate in Europe was recorded (Fig. 7A–C; Starkel et al., 2013). However, the subsequent several-fold reduction in tree ring width may signal a short-term deterioration of ecological conditions, probably related to periodic flooding of the habitat by floodwaters of the Biała Nida River. Interestingly, the age of this pine corresponds to the temporal range of the pine floating chronology from the Podemszczyzna site in the Sandomierz Basin (9980–9830 ±165 mod. cal BP), i.e., the oldest chronology of bog pine in Poland, and Europe (Fig. 7C, site position on Fig. 8 – site 18;

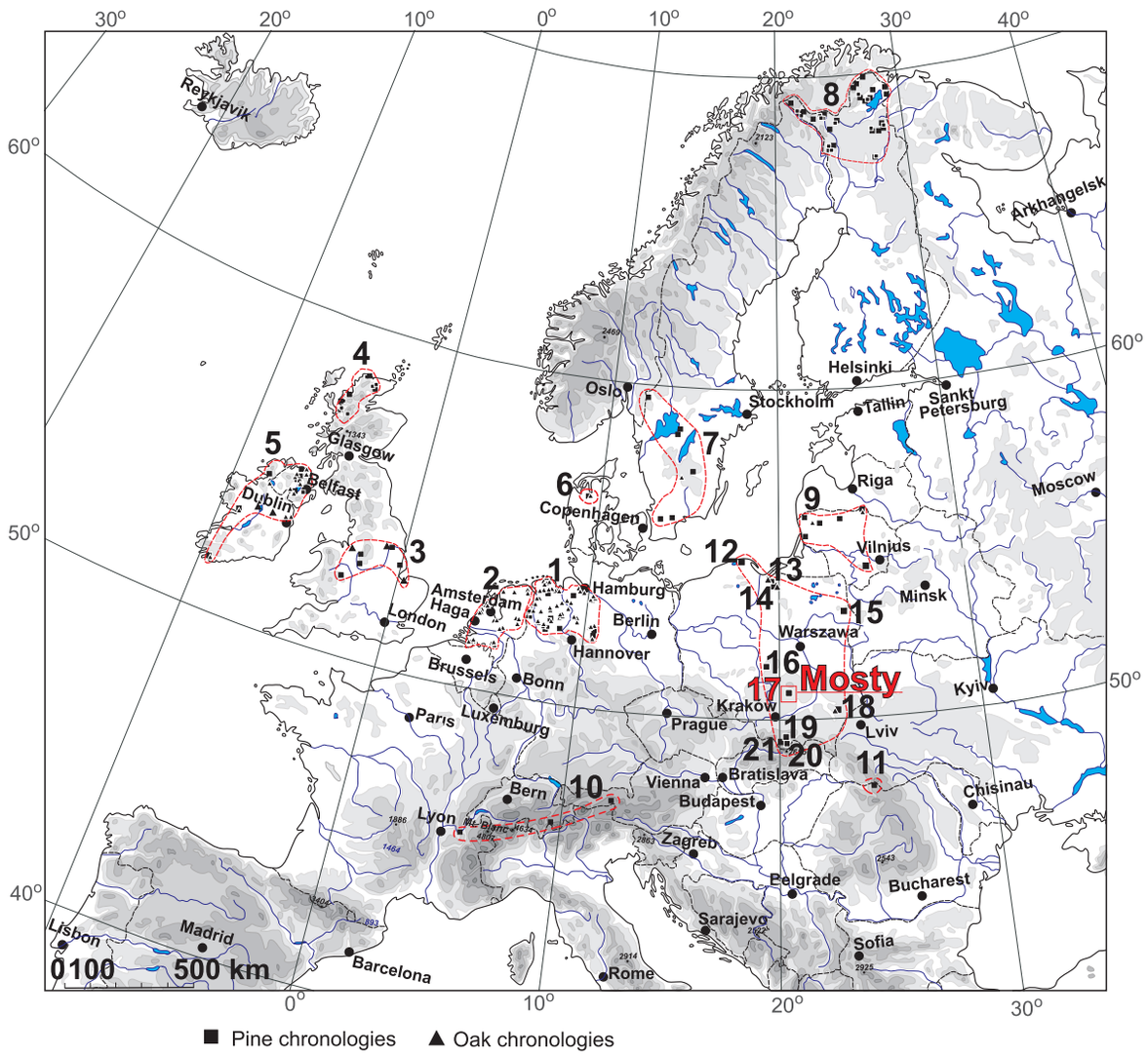

Fig. 8. Location of the Mosty peatland, compared to the location of the other European, and (separately) Polish peatlands with subfossil tree trunks of Scots pine (*Pinus sylvestris*) and oak (*Quercus* sp.)

For site names and authors of chronologies – see Table 4, according to site numbers shown in Figure 7C

Margielewski et al., 2022a) (although older, late-glacial chronologies of pine have been developed, they do not apply to bog pine growing on peatlands – see Dzieduszyńska and Petera-Zganiacz, 2012; Michczyńska et al., 2018). The difference is that the pines from the Podemszczyzna site (which is also a fluviogenic peatland) represent bog pine woodland, while the pine from the Mosty site grew before the formation of the Mosty peatland (Margielewski et al., 2022a).

The trunk of a younger pine tree, occurring in the bottom parts of the organic deposits of the Mosty peatland, fell in ~9426–9128 cal BP (Fig. 2B and Table 1). The course of the tree ring curve also indicates generally good habitat conditions during the tree's growth (Fig. 2B: 3). Thus, like the older pine tree, it grew on the sandy alluvia of the Biała Nida River (there is sand on the trunk), though during the beginning of the Mosty peatland paludification. Brief reductions in its tree ring widths, suggest that it may also have been sporadically subjected to the fluvial activity of the Biała Nida River (Fig. 2A: 3). Both pines, therefore, used to grow in the same place on the Biała Nida floodplain at the bottom of an abandoned shallow meander and certainly do not represent driftwood. Pollen analysis of the bottom sections of peatland deposits indicates a dominance of *Pinus* with some

Picea admixture, and underrepresentation of riparian taxa (Fig. 5). The pines analysed were not part of the riparian forest which usually grows on river floodplains. They could have been remnants of pine forests that grew on alluvial plains during the climatic periods.

Another dated, younger subfossil trunk of Scots pine (*Pinus sylvestris*) dated at ~2964–2632 cal BP fell during ~2815–2632 cal BP. Its tree-ring widths indicate that the onset of its growth (the first 7 rings dated 2964–2782 cal BP) occurred under fa-

Table 4

Sites with dendrochronologically analysed subfossil bog pine (*Pinus sylvestris*), and oak (*Quercus* sp.) in European peatlands (sites: 1–11) and in Polish peatlands (sites 12–21, including the Mosty peatland)

No. of site on Figs. 7 C and 8	Name of site	Tree species	Author(s)
1	Northern Germany	Pine, oak	Leuschner et al. (2007); Eckstein et al. (2011); Achterberg et al. (2017, 2018)
2	Netherlands	Oak	Jansma (1996); Sass-Klassen and Hanraets (2006)
3	England	Pine, oak	Lageard et al. (1999, 2000)
4	Scotland	Pine	Moir et al. (2010); Moir (2012)
5	Ireland	Pine, oak	Pilcher et al. (1995); Torbenson et al. (2015)
6	Denmark	Oak	Edvardsson et al. (2016b)
7	Southern Sweden	Pine	Gunnarson et al. (2003); Gunnarson (2008); Edvardsson (2010); Edvardsson et al. (2012a, b)
8	Finland	Pine	Helama et al. (2004, 2020)
9	Lithuania	Pine, oak	Pukienč (2001); Edvardsson et al. (2016a)
10	Alps	Pine (*Pinus cembra*)	Nicolussi et al. (2005, 2009)
11	Southern Carpathians	stone Pine	Árvai et al. (2016)
	Poland		
12	Krakulice	Pine	Margielewski et al. (2023)
13	Rucianka	Pine, oak	Barniak et al. (2014)
14	Budwity	Pine, oak	Margielewski et al. (2024)
15	Imszar	Pine	Margielewski et al. (2022b)
16	Napoleonów	Pine	Margielewski et al. (2023)
17	Mosty	Pine	this study
18	Podemszczyzna	Pine, oak	Margielewski et al. (2022a)
19	Jezioro Zawadowskie	Fir (*Abies alba*)	Margielewski et al. (2023)
20	Grel	Pine	Margielewski et al. (2022c)
21	Puścizna Wielka	Pine	Krąpiec and Szychowska-Krąpiec (2016); Krąpiec et al. (2016)

vourable ecological conditions, which rapidly deteriorated during the tree's growth. For most of the tree's growth period, the tree rings are extremely narrow (Fig. 2C: 3: compare with growth curves A3 and B3 in Fig. 2). It is very likely that the onset of its growth coincided with marked drainage of the peatland, as indicated by the highly decomposed peat. The sequence of radiocarbon dating and the change in the rate of peat accumulation indicate the possibility of a hiatus occurring here, probably related to the cooling and drying of the climate at ~4.2 ka causing the temporary cessation of peat accumulation. Thus, the tree was likely part of the bog pine woodland that entered the peatland (germination phase) during its extreme desiccation (after 4.2 ka), and then grew for quite a long time under conditions of frequent water table fluctuations in the peatland caused by flooding of the nearby Biała Nida River. The tree falling (tree dying-off phase) was due to frequent floods (causing permanent inundation of the peatland) associated with a significant increase in fluvial and erosional activity of the Biała and Czarna Nida rivers, recorded at the boundary of the Subboreal and Subatlantic phases (2.8 ka event; see Kalicki and Biesaga, 2024). The timing of the germination phase, and tree dying-off phase, correlates well with the floating chronologies of pines in peatlands in Scotland, Finland, Lithuania, the Alps, and also in Polish sites: Rucianka in Warmia region, Imszar in Podlasie, or Puścizna Wielka in the Orawa-Nowy Targ Basin (see Figs. 7C, 8 and Table 4).

The floating chronologies of pine developed (1360–1187 mod. cal BP and 1158–976 mod. cal BP) based on the analysis of tree trunks occurring in the upper parts of the peatland deposits, indicate the occurrence of alternating tree germination and tree dying-off phases (Fig. 3A: 1, B: 1). The course of the averaged dendrochronological curves developed for the floating pine chronologies: 2MOST_A2 and 2MOST_A1, indicates a periodic deterioration of ecological conditions of the habitat, marked by a reduction in tree ring width. For the 2MOST_A2 chronology, this occurred in the periods ~1320–1299 ±27 mod. cal BP; 1275 ±27 mod. cal BP; 1266–1258 ±27 mod. cal BP 1248 ±27 mod. cal BP and after 1222 ±27 mod. cal BP (Fig. 3B). For younger pine chronologies (2MOST_A1) these reductions took place between 1108 and 1074 ± 50 mod cal BP, while long-term reductions, which are simultaneous with tree dying-off phases, were marked in the time intervals 1062–1038 ±50 mod. cal BP and 1004–994 ±50 mod. cal BP (Fig. 3A). The course of tree ring curves with such trends (with alternating germination and dying-off trees phases is typical for bog pine woodlands overgrowing peatlands and was associated with lowering (germination phase) and periodic increase in water level in the peatland, causing dying-off phases of trees (Edvardsson et al., 2016a, b, 2022; Margielewski et al., 2024). Such phenomena have been recorded in peatlands in Europe (e.g., Leuschner et al., 2007; Edvardsson et al., 2016a, b, 2022)

including Poland (Krąpiec et al., 2016; Margielewski et al., 2022a, b, 2024).

The subfossil pine tree trunks that accumulated in the upper part of the Mosty peatland deposits could not have been driftwood transported with the floodwaters of the Biała Nida River, i.e. tree trunks fallen during the undercutting of forest-covered river banks, as was the case of black oaks in the Czarna Nida valley in Wolica (Lindner, 1977), or the Lubrzanka in Cedzynia (Kowalski and Swałdek, 1991), as well as in the Wisła alluvial deposits (Kalicki and Krąpiec, 1995). The meanders were, after all, cut off from the river, and were only locally flooded: either as a result of the river flooding or through a rise in the groundwater table, also related to the river's activity. In the Mosty peatland profile, illuvial horizons appeared in peats, which in various organic infills of the palaeomeanders of the Nida River and its tributaries were referred to as "silty peats" (Kalicki and Biesaga, 2024 – see Fig. 1C – site 6). In the Mosty peatland profile, these were never distinct clastic layers (muds, alluvial soils) forming thick interbeds in organic sediments, typical of strong floods (see Kalicki, 2006) or from long-term flooding of peatland (Margielewski, 2018; Fig. 4A, C, D).

Everything indicates that the pines analysed from the Mosty site overgrew the peatland area: both before its formation (~10,198–9757 cal BP; Fig. 2A), and at various stages of its formation: 2964–2632 cal BP and (floating chronologies) 1360–1187 ±27 mod. cal BP and 1158–976 ±50 mod. cal BP (Figs. 2B, C and 3A, B).

Chronologies 2MOST_A2 and 2MOST_A1 are floating chronologies. Developing absolute chronologies based on these chronologies encounters problems because so far there are few sites in Europe with developed pine chronologies for this period (Finland, Lithuania, the Alps, Romania, while in Poland this is currently the only chronology), and, not all of them are absolute chronologies (Fig. 7C and Table 4). The Miyake effect, i.e., a single, rapid increase in ^{14}C content in wood of individual annual rings, observed so far in the calendar years BP: 9126; 7360, 2610, and particularly: 1176–1175, and 956–955 (Miyake et al., 2012, 2013), can also be used to develop an absolute chronology (see Krapiec et al., 2021). However, this requires further research and funding.

CONCLUSIONS

Within the deposits of the Mosty fluviogenic peatland (southern Poland), palaeoenvironmental changes have been recorded in the interfluve of the Czarna and Biała Nida rivers, occurring from the Boreal phase of the Holocene to the present. The formation of the peatland (developed as sedge peats 1.54 m thick) in the abandoned palaeomeander of the Biała Nida River (directly on Plenivistulian sands) began 9258 ±130 mod. cal BP. In the upper Nida valley, this was a phase of common cutting off and paludification of the Biała and Czarna Nida meanders. Dating of subfossil pine trunks found *in situ* in the bottom parts of the succession indicates that the floodplain area (still before peatland formation) was covered with pine forest. In the deposits, a cold and humid climatic event ~8.2 ka cal BP is marked by a flood horizon: a thin illuvial horizon was formed in the peats, and the flood waters delivered significant amounts of metallic elements (Fe, Mn, Cu, Zn, PB) to the peatland, sourced from a natural ore deposit on the nearby Miedzianka Mt.

The long-term supply of clastic sediment to the peatland, and the formation of the illuvial horizon in the peat during the period 7348–5827 cal BP, were associated with increase in climate humidity during the Holocene climatic optimum (~6500–5900 cal BP). The river's fluvial activity is indicated by a sudden increase in the concentration of heavy metal elements in the peat. The distribution of radiocarbon dates and the degree of peat humification indicate the possible presence of a sedimentary hiatus (of undetermined time range), likely caused by marked desiccation of the peatland at ~4.2 ka (a cold, extreme event). The long-term desiccation of the peatland favoured the encroachment of bog pine woodland onto the peatland. This is indicated by a subfossil pine trunk dated to 2964–2632 cal BP, with very narrow tree rings, the fall of which could have been related to the 2.8 ka event, when a phase of particularly intense erosion was recorded in the upper Nida valley.

In the upper parts of the peatland, formed from clayey and highly decomposed peat (in effect reflecting peatland flooding), subfossil pine stumps occur, based on which pine floating chronologies were developed (1360–1187 mod. cal BP and 1158–976 mod. cal BP). These are remnants of bog pine woodland that encroached on the peatland (germination phase) during drying of the peatland. The rising water level in the peatland during the increase in climatic humidity and the flooding of its surface by shallow floodwaters from the Biała Nida River (as indicated only by illuvial levels in the peat, in the absence of clastic levels typical of strong floods) resulted in tree dying-off phases and falling tree stumps, which were later buried in the sediments. Thus, subfossil pine wood buried in the Mosty peatland deposits was associated with the pine woodland that covered the floodplain of the Nida River (before peatland formation), and bog pine woodland, developed in various stages of peatland formation.

Acknowledgements. This study was supported with funds from the National Science Centre, Poland, grant No. 2017/25/B/ST10/02439 (2018–2022), the statutory work of the Institute of Nature Conservation Polish Academy of Sciences in Krakow, and the statutory work of the AGH University of Krakow, grant No. 16.16.140.315. The authors would like to cordially thank the reviewers: P. Barta, and anonymous reviewer, for theirs valuable comments, which significantly improved the article. The authors would also like to thank the Management of the Organic Fertilizer Production Plant and Sand Mining Plant (Z.W.P. Mosty) in Chęciny for allowing the research to be carried out in the Mosty peat bog and for their assistance in the research conducted.

REFERENCES

Achterberg, I.E.M., Frechen, M., Bauerochse, A., Eckstein, J., Leuschner, H.H., 2017. The Göttingen tree-ring chronologies of peat – preserved oaks and pines from Northeast Germany. Zeitschrift der Deutschen Gesellschaft für Geowissenschaften, **168**: 9–19; https://doi.org/10.1127/zdgg/2016/0042

Achterberg, I.E.M., Eckstein, J., Birkholz, B., Bauerochse, A., Leuschner, H.H., 2018. Dendrochronogically dated pine stumps document phase wise bog expansion at a northwest German site between c. 6700 BC and c. 3400 BC. Climate of the Past, **14**: 85–100; https://doi.org/10.5194/cp-14-85-2018

Árvai, M., Popa, I., Mîndrescu, M., Nagy, B., Kern, Z., 2016. Dendrochronology and radiocarbon dating of subfossil conifer logs from a peat bog, Maramureş Mts., Romania. Quaternary International, **415**: 6–14; https://doi.org/10.1016/j.quaint.2015.11.066

Baillie, M.G.L, Pilcher, J.R., 1973. A simple cross-dating program for tree-ring research. Tree-Ring Bulletin, **33**: 7–14.

Barniak, J., Krąpiec, M., Jurys, L., 2014. Subfossil wood from the Rucianka raised bog (NE Poland) as an indicator of climatic changes in the first millennium BC. Geochronometria, **41**: 104–110; https://doi.org/10.2478/s13386-013-0126-5

Becker, B., Schirmer, W., 1977. Palaeoecological study on the Holocene valley development of the River Maine, southern Germany. Boreas, **6**: 303–321; https://doi.org/10.1111/j.1502-3885.1977.tb00296.x

Berglund, B.E., Ralska-Jasiewiczowa, M., 1986. Pollen analysis and pollen diagrams. In: Handbook of Holocene Palaeoecology and Palaeohydrology (ed. B.E. Berglund): 455–484. John Wiley & Sons, Chichester.

Bond, G., Showers, W., Cheseby, M., Lotti, R., Almasi, P., Domenocal, P., Priore, P., Cullen, M., Hajdas, I., Bonani, G., 1997. A pervasive millennial – scale cycle in North Atlantic Holocene and global climates. Science, **278**: 1257–1266; https://doi.org/10.1126/science.278.5341.1257

Bond, G., Evans, M.N., Muscheler., 2008. North Atlantic Holocene Drift Ice Proxy Data. IGBP PAGES/World Data Center for Paleoclimatology Data Contribution Series # 2008-018. NOAA/NCDC Paleoclimatology Program, Boulder CO, USA. Found at: ftp://ftp.ncdc.noaa.gov/pub/data/paleo/contributions_by_author/bond2001/bond2001.txt, accessed January 8th, 2019.

Borówka, R.K., Tomkowiak, J., Okupny, D., Forysiak, J., 2015. Chemical composition of biogenic sediments from the river valley Luciąża (Bęczkowice peatland in the Piotrków Plain) (in Polish with English summary). Folia Quaternaria, **83**: 5–23; https://doi.org/10.1515/folquart -2015-0004

Bronk Ramsey, C., 2009. Bayesian analysis of radiocarbon dates. Radiocarbon, **51**: 337–360; https://doi.org/10.2458/azu_js_rc.51.3494

Bronk Ramsey, C., 2017. Methods for summarizing radiocarbon datasets. Radiocarbon, **59**: 1809-1833; https://doi.org/10.1017/RDC.2017.108

Carozza, J-M., Carozza, L., Valette, P., Llubes, M., Py, V., Galop, D., Danu, M., Ferdinand, L., David, M., Sévégnes, L., Bruxelles, L., Jarry, M., Duranthon, F., 2014. The subfossil tree deposits from the Garonne Valley and their implications on Holocene alluvial plain dynamics. Comptes Rendus Geoscience, **346**: 20–27; http://dx.doi.org/10.1016/j.crte.2014.01.001

Damman, A.W.H., 1978. Distribution and movement of elements in ombrotrophic peat bogs. Oikos, **30**: 480–495; https://doi.org/10.2307/3543344

Davison, W., 1993. Iron and manganese in lakes. Earth-Science Reviews, **34:** 119–163; https://doi.org/10.1016/0012-8252(93)90029-7

Dzieduszyńska, D., Petera-Zganiacz, J., 2012. Geologic position of the Younger Dryas subfossil forest in the Warta River valley, central Poland. Bulletin of the Geological Society of Finland, **84**: 69–79.

Dzierżek, J., Lindner, L., Cabalski, K., 2019. Quaternary valley levels and river terraces in the Western part of the Holy Cross Mountains. Studia Quaternaria, **36**: 109–118; https://doi.org/10.24425/sq.2019.126383

Eckstein, D., Bauch, J., 1969. Beitrag zur Rationalisierung eines dendrochronologischen Verfahrens und zur Analyse seiner Aussagesicherheit. Forstwissenschaftliches Centralblatt, **88**: 230–250.

Eckstein, J., Leuschner, H.H., Bauerochse, A., 2008. Dendroecological studies on subfossil pine and oak from Totes Moor near Hannover (Lower Saxony, Germany). TRACE, **6**: 70–76.

Eckstein, J., Leuschner, .HH., Bauerochse, A., 2011. Mid-Holocene pine woodland phases and mire development – significance of dendroecological data from subfossil trees from northwest Germany. Journal of Vegetation Science, **22**: 781–794; https://doi.org/10.1111/j.1654-1103.01283

Edvardsson, J., 2010. Development of south Swedish pine chronologies from peat bogs – extension of existing records and assessment of palaeoclimatic potential. TRACE, **8**: 124–129; https://doi.org/10.2312/GFZ.b103-10058

Edvardsson, J., Leuschner, H.H., Linderson, H., Linderholm, H.W., Hammarlund, D., 2012a. South Swedish bog pines as indicators of mid-Holocene climate variability. Dendrochronologia, **30**: 93–103; https://doi.org/10.1016/j.dendro.2011.02.003

Edvardsson, J., Linderson, H., Rundgren, M., Hammarlund, D., 2012b. Holocene peatland development and hydrological variability inferred from bog-pine dendrochronology and peat stratigraphy – a case study from southern Sweden. Journal of Quaternary Science, **27**: 553–563; https://doi.org/10.1002/jqs.2543

Edvardsson, J., Corona, C., Mazeika, J., Pukienč, R., Stoffel, M., 2016a. Recent advances in long-term climate and moisture reconstructions from the Baltic region: Exploring the potential for a new multi-millenial tree-ring chronology. Quaternary Science Reviews, **131**: 118–126; https://doi.org/10.1016/j.quascirev.2015.11.005

Edvardsson, J., Stoffel, M., Corona, C., Bragazza, L., Leuschner, H.H., Charman, D.J., Helama, S., 2016b. Subfossil peatland trees as proxies for Holocene palaeohydrology and palaeoclimate. Earth – Science Reviews, **163**: 118–140; https://doi.org/10.1016/j.earscirev.2016.10.005

Edvardsson, J., Helama, S., Rundgren, M., Nielsen, A.B., 2022. The integrated use of dendrochronological data and paleoecological records from northwest European peatland and lakes for understanding long–term ecological and climate changes – a review. Frontiers in Ecology and Evolution, **10**, 781882; https://doi.org/10.3389/fevo.2022.781882

Finsinger, W., Dos Santos, T., McKey, D., 2013. Estimating variation in stomatal frequency at intra-individual, intra-site, and inter-taxonomic levels in populations of the *Leonardoxa africana* (Fabaceae) complex over environmental gradients in Cameroon. Compte Rendu Geoscience, **345**: 350–359.

Florescu, G., Brown, K.J., Carter, V.A., Kunes, P., Veski, S., Feuerdan, A., 2019. Holocene rapid climate changes and ice-rafting debris events reflected in high-resolution European charcoal records. Quaternary Science Reviews, **222**, 105877; https://doi.org/10.1016/j.quascirev.2019.105877

Gilewska, S., 1972. Wyżyny Śląsko-Małopolskie (in Polish). In: Geomorfologia Polski (ed. M. Klimaszewski): 232–339. PWN, Warszawa.

Grimm, E.C., 1987. CONISS: a Fortran 77 program for stratigraphically constrained cluster analysis by the method of incremental sum of squares. Computer & Geosciences, **13**: 13–35; https://doi.org/ 10.1016/0098-3004(87)90022-7

Grimm, E.C., 1991. TILIA and TILIA Graph. Illinois State Museum, Springfield.

Gunnarson, B.E., 2008. Temporal distribution pattern of subfossil pines in central Sweden: perspective on Holocene humidity fluc-

tuations. The Holocene, **18**: 569–577; https://doi.org/10.1177/0959683608089211

Gunnarson, B.E., Borgmark, A., Wastegård, S., 2003. Holocene humidity fluctuations in Sweden inferred from dendrochronology and peat stratigraphy. Boreas, **32:** 347–360; https://doi.org/10.1111/j.1502-3885.2003.tb01089.x

Hakenberg, M., 1974. Objaśnienia do Szczegółowej Mapy Geologicznej Polski 1:50 000, arkusz Chęciny (850). Reambulacja: Złonkiewicz, Z., 2013 (in Polish). Państwowy Instytut Geologiczny, Warszawa.

Hakenberg, M., 1978. Albian–Cenomanian palaeotectonics and palaeogeography of the Miechów Depression, northern part (in Polish with English summary). Studia Geologica Polonica, **58**: 1–104.

Hakenberg, M., Lindner, L., 1971. Quaternary deposits of the middle Nida valley (in Polish with English summary). Acta Geologica Polonica, **21**: 241–263.

Heiri, O., Lotter, A.F., Lemcke, G., 2001. Loss on ignition as a method for estimating organic and carbonate content in sediments: reproducibility and comparability of results. Journal of Paleolimnology, **25**: 101–110. https://doi.org/10.1023/A:1008119611481

Helama, S., Lindholm, M., Timonen, M., Eronen, M., 2004. Dendrochronologically dated changes in the limit of pine in northernmost Finland during the past 7.5 millennia. Boreas, **33**: 250–259; https://doi.org/10.1111/j.1502-3885.2004.tb01145.x

Helama, S., Kuoppama, M., Sutinen, R., 2020. Subaerially preserved remains of pine stemwood as indicators of late Holocene timberline fluctuation in Fennoscandia, with comparison of tree ring and ^{14}C dated depositional histories of subfossil trees from dry and wet sites. Review of Palaeobotany and Palynology, **278,** 104223; https://doi.org/104223. 10.1016/j.revpalbo.2020.104223

Holmes, R.L., 1999. Users Manual for Program COFECHA. University of Arizona, Tuscon.

Hupp, C., 2000. Hydrology, geomorphology, and vegetation of Coastal Plain rivers in the southeastern United States. Hydrological Processes, **14**: 2991–3010; https://doi.org/10.1002/1099-1085(200011/12)14:16/173.0.CO;2-H

Ivy-Ochs, S., Kerschner, H., Maisch, M., Christl, M., Kubik, P.W., Schlüchter, C., 2009. Latest Pleistocene and Holocene glacier variations in the European Alps. Quaternary Science Reviews, **28**: 2137–2149; https://doi.org/10.1016/j.quascirev.2009.03.009

Jansma, E., 1996. An 1100-year tree-ring chronology of oak for the Dutch coastal region. In: Tree-Rings, Environment and Humanity – Proceedings of the International Tree-Ring Conference 1995 (eds. J.S. Dean, D.M. Meko and T.W. Swetnam): 769–778. University of Arizona.

Juggins, S., 2022. riojaPlot: Stratigraphic Diagrams in R, Package Version 0.1-20; https://github.com/nsj3/riojaPlot

Kalicki, T., 2006. Reflection of climatic changes and human activity and their role in the Holocene evolution of Central European valleys (in Polish with English summary). Prace Geograficzne, **204**.

Kalicki, T., Biesaga, P. (eds.), 2024. Evolution of the Nida River Valley during the Late Glacial and Holocene (in Polish with English summary). Monografie Geografia, Geoarcheologia, **2**: 1–147.

Kalicki, T., Krąpiec, M., 1995. Problems of dating alluvium using buried subfossil tree trunk: lesson from the black oaks of the Vistula Valley, Central Europe. The Holocene, **5**: 243–250; https://doi.org/10.1177/095968369500500213

Kalicki, T., Przepióra, P., Kusztal, P., Chrabąszcz, M., Fularczyk, K., Kłusakiewicz, E., Frączek, M., 2020. Historical and present-day human impact on fluvial systems in the Old-Polish Industrial District (Poland). Geomorphology, **357**, 107062; https://doi.org/10.1016/j.geomorph.2020.107062

Kaniewski, D., Marriner, N., Cheddadi, R., Guiot, J., VanCampo, E., 2018. The 4.2 ka BP event in Levant. Climate of the Past, **14**: 1529–1542; https://doi.org/10.5194/cp-14-1529-2018

Klimek, K., 1974. The structure and mode sedimentation of the flood-plain deposits in the Wisłoka valley (South Poland). Studia Geomorphologica Carpatho-Balcanica, **8**: 136–151.

Knighton, D., 1998. Fluvial Forms and Processes. Arnold, London.

Kolář, T., Rybniček, M., 2011. Dendrochronological and radiocarbon dating of subfossil wood from the Morava River basin. Geochronometria, **38**: 155–161; https://doi.org/10.2478/s13386-011-0021-x

Kołaczek, P., Buczek, K., Margielewski, W., Gałka, M., Rycerz, A., Woszczyk, M., Karpińska-Kołaczek, M., Marcisz, K., 2021. Development and degradation of a submontane forest in the Beskid Wyspowy Mountains (Polish Western Carpathians) during the Holocene. The Holocene, **31**: 1716–1732; https://doi.org/10.1177/09596836211033200

Kondracki, J., 2000. Geografia regionalna Polski (in Polish). PWN, Warszawa.

Kowalski, B., 2002. Geneza i wiek osadów terasy zalewowej i nadzalewowej (wysokiej) środkowego odcinka doliny Lubrzanki w Górach Świętokrzyskich (in Polish). Prace Instytutu Geografii Akademii Świętokrzyskiej, **8**: 151–216.

Kowalski, B., Swałdek, M., 1991. Age of flood terrace deposits and Holocene development of Lubrzanka River Valley, the Cedzyna region the Holy Cross Mountains (in Polish with English summary). Przegląd Geologiczny, **39**: 166–172.

Kozłowski, J.K., Kaczanowski, P., 1998. Najdawniejsze dzieje ziem polskich (in Polish). Wydaw. Fogra, Kraków.

Krawczyk, A., Krąpiec, M., 1995. Dendrochronologiczna baza danych (in Polish). Materiały II Krajowej Konferencji: Komputerowe wspomaganie badań naukowych: 247–252. Wrocławskie Towarzystwo Naukowe, Wrocław.

Krąpiec, M., Szychowska-Krąpiec, E., 2016. Subfossil bog-pine chronology from the Puścizna Wielka raised bog, Orawa Basin, southern Poland. Quaternary International, **415**: 145–153; https://doi.org/10.1016/j.quaint.2015.12.045

Krąpiec, M., Walanus, A., 2011. Application of the triple photomultiplier liquid spectrometer Hidex 300SL in radiocarbon dating. Radiocarbon, **53**: 543–550; https://doi.org/10.1017/S0033822200034640

Krąpiec, M., Margielewski, W., Korzeń, K., Szychowska-Krąpiec, E., Nalepka, D., Łajczak, A., 2016. Late Holocene palaeoclimate variability: the significance of bog pine dendrochronology related to peat stratigraphy. The Puścizna Wielka raised bog case study (Orawa–Nowy Targ Basin, Polish Inner Carpathians). Quaternary Science Reviews, **148**: 192–208; https://doi.org/10.1016/j.quascirev.2016.07.022

Krąpiec, M., Rakowski, A., Pawlyta, J., Wiktorowski, D., Bolka, M., 2021. Absolute dendrochronological scale for pine (*Pinus sylvestris* L.) from Ujście (NW Poland), dated using rapid atmospheric ^{14}C changes. Radiocarbon, **63**: 1205–1214; https://doi.org/10.1017/RDC.2020.116

Krupa, J., 2013. Natural and anthropogenic factors influenced Czarna Nida river valley during the Late Glacial and Holocene (in Polish with English summary). Folia Quaternaria, **81**: 5–174.

Krupa, J., 2015. Natural and anthropogenic channel pattern changes in the mid-mountain valley during the Late Glacial and Holocene, Polish Uplands. Quaternary International, **370**: 55–65; https://doi.org/10.1016/j.quaint.2014.12.045

Lageard, J.G.A., Chambers, F.M., Thomas, P.A., 1999. Climatic significance of the marginalization of Scots pine (*Pinus sylvestris* L.) c. 2500 BC at White Moss, south Cheshire UK. The Holocene, **9**: 321–331; https://doi.org/10.1191/095968399674220353

Le Roy, M., Ivy-Ochs, S., Nucolussi, K., Monegato, G., Reitner, J.M., Colucci, R.R., Ribolini, A., Spagnolo, M., Stoffel, M., 2024. Holocene glacier variations in the Alps. In: European Gla-

cial Landdscapes. The Holocene (eds. D. Palacios, P.D. Hughes, V. Jomell and L.M. Tanarro): 367–418, Elsevier; https://doi.org/10.1016/B978-0-323-99712-6.00018-0

Leuschner, H.H., Bauerochse, A., Metzler, A., 2007. Environmental change, bog history and human impact around 2900 B.C. in NW Germany – preliminary results from a dendroecological study of a sub-fossil pine woodland at Campemoor, Dümmer Basin. Vegetation History and Archaeobotany, **16**: 183–195; https://doi.org/10.1007/s00334-006-0084-4

Lézine, A.M., Holl, A.F.C., Lebamba, J., Vincens, A., Assi-Khaudjis, C., Fevrier, L., Sultan, E., 2013. Temporal relationship between Holocene human occupation and vegetation change along the northwestern margin of the Central African rainforest. Compte Rendu Geoscience, **345**: 327–335; https://doi.org/10.1016/j.crte.2013.03.001

Lindner, L., 1977. The age of river flood-terraces from the Góry Świętokrzyskie Mts. in the light of ^{14}C datings of the "black oak horizons" (in Polish with English summary). Kwartalnik Geologiczny, **21**: 325–335.

Lindner, L., 1978. Palaeogeomorphologic evolution of the western part of the Holy Cross region in Pleistocene (in Polish with English summary). Rocznik Polskiego Towarzystwa Geologicznego, **48**: 479–508.

Lindner, L., 1982. South-Polish glaciations (Nidanian, Sanian) in southern Central Poland. Acta Geologica Polonica, **32**: 163–177.

Ludwikowska-Kędzia, M., 2000. Evolution of the Middle Segment of the Belnianka River Valley in the Late Glacial and Holocene. Dialog Press, Warszawa.

Magny, M., 2013. Orbital, ice-sheet, and possible solar forcing of Holocene lake-level fluctuations in west-central Europe: a comment on Bleicher. The Holocene, **23**: 1202–1212; https://doi.org/10.1177/0959683613483627

Magny, M., Begeot, C., Guiot, J., Peyron, O., 2003. Contrasting patterns of hydrological changes in Europe in response to Holocene climate cooling phases. Quaternary Science Reviews, **22**: 1589–1596; https://doi.org/10.1016/S0277-3791(03)00131-8

Mangerud, J., Andersen, S.T., Berglund, B., Donner, J.J., 1974. Quaternary stratigraphy of Norden, a proposal for terminology and classification. Boreas, **3**: 109–126; https://doi.org/10.1111/j.1502-3885.1974.tb00669.x

Margielewski, W., 2018. Landslide fens as a sensitive indicator of the palaeoenvironmental changes since the Late Glacial; Polish Western Carpathians case study. Radiocarbon, **60**: 1199–1213; https://doi.org/10.1017/RDC.2018.68

Margielewski, W., Krąpiec, M., Buczek, K., Korzeń, K., Szychowska-Krąpiec, E., Pociecha, A., Pilch, J., Obidowicz, A., Sala, D., Klimek, A., 2022a. Bog pine and deciduous trees chronologies related to peat sequences stratigraphy of the Podemszczyzna peatland (Sandomierz Basin, South-Eastern Poland). Radiocarbon, **64**: 1557–1575; https://doi.org/10.1017/RDC.2022.38

Margielewski, W., Krąpiec, M., Kupryjanowicz, M., Fiłoc, M., Buczek, K., Stachowicz-Rybka, R., Obidowicz, A., Pociecha, A., Szychowska-Krąpiec, E., Sala, D., Klimek, A., 2022b. Bog pine dendrochronology related to peat stratigraphy: Palaeoenvironmental changes reflected in peatland deposits since the Late Glacial (case study of the Imszar raised bog, Northeastern Poland). Quaternary International, **613**: 61–80; https://doi.org/10.1016/j.quaint.2021.11.007

Margielewski, W., Michczyńska, D.J., Buczek, K., Michczyński, A., Korzeń, K., Obidowicz, A., 2022c. Towards the understanding of the present-day human impact on peatland deposits formed since the Late Glacial: a "retrospective" age-depth model of the Grel raised bog (Polish Inner Carpathians). Radiocarbon, **64**: 1525–1543; https://doi.org/10.1017/RDC.2022.62

Margielewski, W., Krąpiec, M., Korzeń, K., Buczek, K., Kupryjanowicz, M., Fiłoc, M., Stachowicz-Rybka R., Kołaczek, P., Niska, M., Wojtal, A.Z., Szychowska-Krąpiec, E., Obidowicz, A., Barniak, J., Gałka, M., Pociecha, A., Mroczkowska, A., Sala, D., Urban, J., Pilch, J., 2023. Bog pine dendrochronology related to peat stratigraphy: reconstruction of the Holocene palaeoenvironmental changes in the territory of Poland on the basis of dendrochronological studies of subfossil trees and peat multiproxy analysis. XXI Congress INQUA, Rome, 13–20 July 2023, Rome, Italy: 1198–1199.

Margielewski, W., Krąpiec, M., Buczek, K., Szychowska-Krąpiec, E., Korzeń, K., Niska, M., Stachowicz-Rybka, R., Wojtal, A.Z., Mroczkowska, A., Obidowicz, A., Sala, D., Drzewicki, W., Barniak, J., Urban, J., 2024. Hydrological variability of middle European peatland during the Holocene, inferred from subfossil bog-pine and bog oak dendrochronology and high-resolution peat multiproxy analysis: the Budwity peatland (northern Poland). Science of The Total Environment, **931**, 172925; https://doi.org/10.1016/j.scitotenv.2024.172925

Matuszkiewicz, W., Faliński, J.B., Kostrowicki, A.S., Matuszkiewicz, J.M., Olaczek, R., Wojterski, T., 1995. Potencjalna roślinność naturalna Polski. Mapa przeglądowa 1:300 000, arkusz C3 (in Polish). IGIPZ PAN, Warszawa.

Mazurek, M., Dobrowolski, R., Osadowski, Z., 2014. Geochemistry of deposits from spring-fed fens in West Pomerania (Poland) and its significance for palaeoenvironmental reconstruction. Geomorphologie, **4**: 323–342; https://doi.org/10.4000/geomorphologie.10765

McCay, N., Kaufman, D.S., Arcusa, S.H., Kolus, H.R., Edge, D.C., Erb, D.C., Hancock, C.L., Routson, C.C., Żarczyński, M., Marschall, L.P., Roberts, G.K., Telles, F., 2024. The 4.2 ka events is not remarkable in the context of Holocene climate variability. Nature Communications, **15**, 6555; https://doi.org/10.1038/s41467-024-50886-w

Michczyńska, D.J., Krapiec, M., Michczyński, A., Pawlyta, J., Goslar, T., Nawrocka, N., Piotrowska, N., Szychowska-Krąpiec, E., Waliszewska, B., Zborowska, M., 2018. Different pretreatment methods for ^{14}C dating of Younger Dryas and Allerød pine wood (*Pinus sylvestris* L.). Quaternary Geochronology, **48**: 38–44; https://doi.org/10.1016/j.quageo.2018.07.013

Miyake, F., Nagaya, K., Masuda, K., Nakamura, T., 2012. A signature of cosmic-ray increase in AD 774-775 from tree rings in Japan. Nature, **486**: 240–242; https://doi.org/10.1038/nature11123

Miyake, F., Masuda, K., Nakamura, T., 2013. Another rapid event in the carbon-14 content of tree rings. Nature Communications, **4**, 1748; https://doi.org/10.1038/ncomms2783

Moir, A., 2012. Development of a Neolithic pine tree-ring chronology for northern Scotland. Journal of Quaternary Science, **27**: 503–508; https://doi.org/10.1016/j.revpalbo.2018.03.005

Moir, A.K., Leroy, S.A.G., Brown, D., Collins, P.E.F., 2010. Dendrochronological evidence for a lower water-table on peatland around 3200-3000 BC from subfossil pine in northern Scotland. Holocene, **20**: 931–942; https://doi.org/10.1177/0959683610365935

Nicolussi, K., Kaufmann, M., Patzelt, G., van der Plicht, J., Thurner, A., 2005. Holocene tree-line variability in the Kauner Valley, Central Eastern Alps, indicated by dendrochronological analysis of living trees and subfossil logs. Vegetation History and Archaeobotany, **14**: 221–234; https://doi.org/10.1007/s00334-005-0013-y

Nicolussi, K., Kaufmann, M., Melvin, T.M., van der Plicht, J., Schießling, P., Thurner, A., 2009. A 9111 year long conifer tree-ring chronology for the European Alps: a base for environ-

mental and climatic investigations. The Holocene, **19**: 909–920; https://doi.org/10.1177/0959683609336565

Pabian, G., Kalicki, T., Przepióra, P., 2022. Traces of historical copper mining and metallurgical activity preserved in the relief and sediments in Miedzianka region (Holy Cross Mts., Poland). In: Sbornik abstraktů 27. Kvartér Ústav geologických věd PrF MU a Česká geologická společnost (eds. A. Plichta, T. Turek, N. Dubjelova and M. Ivanov): 32. Brno.

Pánek, T., Smolková, V., Hradecký, J., Baroň, I., Šilhán, K., 2013. Holocene reactivations of catastrophic complex flow-like landslides in the Flysch Carpathians (Czech Republic Slovakia). Quaternary Research, **80**: 33–46; https://doi.org/10.1016/j.yqres.2013.03.009

Panin, A.V., Sidorchuk, A.Y., Chernov, A.V., 1999. Historical background to floodplain morphology: examples from the east European Plain. Geological Society Special Publications, **163**: 217–229.

Pansu, M., Gautheyrou, J., 2006. Handbook of Soil Analysis. Mineralogical, Organic and Inorganic Methods. Springer, Berlin.

Pawełczyk, F., Michczyński, A., Tomkowiak, J., Tudyka, K., Fagel, N., 2018. Mid to Late Holocene element al record and isotopic composition of lead in a peat core from Wolbrom (S Poland). Mires and Peat, **21**: 1–13; https://doi.org/10.19189/MaP.2018.OMB.349

Pilcher, J.R., Baillie, M.G.L., Brown, D.M., McCormac, Macsweeney, P.B., Mclawrence, A.S., 1995. Dendrochronology of subfossil pine in the north of Ireland. Journal of Ecology, **83**: 665–672; https://doi.org/10.2307/2261634

Posit team, 2025. RStudio: Integrated Development Environment for R. Posit Software, PBC, Boston, MA.

Przepióra, P., Kalicki, T., Podrzycki, Ł., Zubek, K., 2024. Record of bloomeries activity in the alluvium of the central Czarna Nida River (Świętokrzyskie Voivodeship) – case study. Acta Universitatis Lodziensis, Folia Geographica Physica, **23**: 7–18; https://doi.org/10.18778/1427-9711.23.01

Przychodni, A., 2006. Starożytne hutnictwo nad Nidą jako potencjalna enklawa świętokrzyskiego centrum dymarskiego (in Polish). In: 50 lat badań nad starożytnym hutnictwem świętokrzyskim (eds. S. Orzechowski and I. Suliga): 103–123. Archeologia–Metalurgia–Edukacja, Kielce. Wydaw. Państwowego Muzeum Archeologicznego, Warszawa.

Pukienč, R., 2001. Natural change in bog vegetation reconstructed by sub-fossil tree remnant analysis. Biologija, **2**: 111–113.

Reimer, P., Austin, W., Bard, E., Bayliss, A., Blackwell, P., Bronk Ramsey, C., Butzin, M., Cheng, H., Edwards, R., Friedrich, M., Grootes, P., Guilderson, T., Hajdas, I., Heaton, T., Hogg, A., Hughen, K., Kromer, B., Manning, S., Muscheler, R., Palmer, J., Pearson, C., van der Plicht, J., Reimer, R., Richards, D., Scott, E., Southon, J., Turney, C., Wacker, L., Adolphi, F., Büntgen, U., Capano, M., Fahrn, S., Fogtmann-Schulz, A., Friedrich, R., Köhler, P., Kudsk, S., Miyake, F., Olsen, J., Reinig, F., Sakamoto, M., Sookdeo, A., Talamo, S., 2020. The IntCal20 Northern Hemisphere radiocarbon age calibration curve (0–55 cal. ka BP). Radiocarbon, **62**: 725–757; https://doi.org/10.1017/RDC.2020.41

Rinn, F., 2005. TSAP-Win. Time series analysis and presentation for dendrochronology and related applications. User Reference. RINNTECH GMBH, Heidelberg, Germany.

Rubinowski, Z., 1971. The non-ferrous metals ores of the Świętokrzyskie Mountains and their metallogenic position (in Polish with English summary). Biuletyn Instytutu Geologicznego, **247**: 1–166.

Rutkowski, J., 1996. Geologia Niecki Nidziańskiej (in Polish). Studia Ośrodka Dokumentacji Fizjograficznej, **14**: 35–61.

Sass-Klassen, U., Hanraets, E., 2006. Woodlands in the past – the excavation of wetland woods at Zwolle-Sadshagen (the Netherlands): growth pattern and population dynamics of oak and ash. Netherland Journal of Geosciences, **85**: 61–71; https://doi.org/10.1017/S0016774600021429

Skripkin, V.V., Kovalyukh, N.N., 1998. Recent developments in the procedures used at the SSCER Laboratory for the routine preparation of lithium carbide. Radiocarbon, **40:** 211–214; https://doi.org/10.1017/S0033822200018063

Starkel, L., Kalicki, T., Krąpiec, M., Soja, R., Gębica, P., Czyżowska, E., 1996. Hydrological changes of valley floors in the upper Vistula basin during Late Glacial and Holocene. Geographical Studies, Special Issue, **9**: 7–128.

Starkel, L., Michczyńska, D., Krąpiec, M., Margielewski, W., Nalepka, D., Pazdur, A., 2013. Progress in the Holocene chrono-climatostratigraphy of Polish territory. Geochronometria, **40**: 1–21; https://doi.org/10.2478/s13386-012-0024-2

Suligowski, R., Kupczyk, E., Kasprzyk, A., Koślacz, R., 2009. Woda w środowisku przyrodniczym województwa świętokrzyskiego (in Polish). Wydaw. Instytutu Geografii UJK, Kielce.

Swęd, M., Urbanek, P., Krechowicz, I., Dworczak, P., Wiecka, P., Mleczak, M., Tobys, P., 2015. Mineralogy of weathering heaps in the Miedzianka deposits (Holy Cross Mountains) (in Polish with English summary). Przegląd Geologiczny, **63**: 363–370.

Szczepanek, K., 1961. The history of the late glacial and Holocene vegetation of the Holy Cross Mountains (in Polish with English summary). Acta Palaeobotanica, **2**: 1–45.

Szczepanek, K., 1982. Development of the peat-bog at Słopiec and the vegetational history of the Świętokrzyskie (Holy Cross) Mts. in the last 10 000 years. Acta Palaeobotanica, **22**: 117–130.

Śnieszko, Z., 1978. Holoceńskie zmiany w środowisku naturalnym dna doliny Czarnej i Białej Nidy na obszarze projektowanego zbiornika Chęciny rejon wsi Mosty–Żerniki (in Polish). Archiwum IA WUOZ, Kielce.

Teisseyre, A.K., 1988. Recent overbank deposits of Sudetic Valleys, SW Poland. Part II: selected methodological problems (in Polish with English summary). Geologia Sudetica, **23**: 66–95.

Tołpa, S., Jasnowski, M., Pałczyński, A., 1971. New classification of peat based on phytosociological methods. Bulletin International Peat Society, **2**: 9–14.

Torbenson, C.A., Plunkett, G., Brown, D.N., Pilcher, J.R., Leuschner, H.H., 2015. Asynchrony in key Holocene chronologies: Evidence from Irish bog pines. Geology, **43**: 799–802; https://doi.org/10.1130/G36914.1

Vandenberghe, J., Kaase, C., Bohncke, S., Kozarski, S., 1994. Climate-related river activity at the Weichselian-Holocene transition: a comparative study of the Warta and Maas rivers. Terra Nova, **6**: 476–485; https://doi.org/10.1111/j.1365-3121.1994.tb00891.x

Walker, M., Gibbard, P., Head, M.J., Berkelhammer, M., Björck, S., Cheng, H., Cwynar, L.C., Fisher, D., Gknis, V., Long, A., Lowe, J., Newnham, R., Rasmussen, S.O., Weiss, H., 2019. Formal subdivision of the Holocene series/epoch: a summary. Journal Geological Society of India, **93**: 135–141; https://doi.org/10.1002/jqs.2565

Wanner, H., Solomina, O., Grosjean, M., Ritz, S.P., Jetel, M., 2011. Structure and origin of Holocene cold events. Quaternary Science Reviews, **30**: 3109–3123; https://doi.org/10.1016/j.quascirev.2011.07.010

Wanner, H., Mercolli, L., Grosjean, M., Ritz, S.P., 2015. Holocene climate variability and change: a data based review. Journal of the Geological Society, **172**: 254–263; https://doi.org/10.1144/jgs2013-101

Zielski, A., Krąpiec, M., 2004. Dendrochronology (in Polish with English summary). Wydaw. Naukowe PWN, Warszawa.